

August 1, 2000

Developments in Rare Kaon Decay Physics*

A.R. Barker

Department of Physics, University of Colorado, Boulder, Colorado 80309;
e-mail: tonyb@cuhep.colorado.edu

S.H. Kettell

Physics Department, Brookhaven National Laboratory, Upton, New York 11973;
e-mail: kettell@bnl.gov

KEYWORDS: *CP* violation, CKM matrix, lepton flavor violation

ABSTRACT: We review the current status of the field of rare kaon decays. The study of rare kaon decays has played a key role in the development of the standard model, and the field continues to have significant impact. The two areas of greatest import are the search for physics beyond the standard model and the determination of fundamental standard-model parameters. Due to the exquisite sensitivity of rare kaon decay experiments, searches for new physics can probe very high mass scales. Studies of the $K \rightarrow \pi \nu \bar{\nu}$ modes in particular, where the first event has recently been seen, will permit tests of the standard-model picture of quark mixing and *CP* violation.

CONTENTS

INTRODUCTION	2
<i>Standard Model "Golden Modes" and CKM Matrix</i>	3
<i>Form Factor Measurements</i>	5
<i>Searches for New Physics</i>	5
<i>CP</i> VIOLATION AND THE CKM MATRIX	6
$K_L^0 \rightarrow \mu^+ \mu^-$	7
$K_L^0 \rightarrow \pi^0 \ell^+ \ell^-$	9
$K \rightarrow \pi \nu \bar{\nu}$	11
FORM FACTORS	16
$K_L^0 \rightarrow \gamma \gamma$ and Related Decays	17
$K \rightarrow \pi \gamma \gamma$	20
$K^+ \rightarrow \pi^+ \ell^+ \ell^-$	21
$K \rightarrow \pi \pi \gamma$	22
Radiative $K_{\ell 2}$ Decays	24
$K \rightarrow \pi \pi \nu_e$	25
Other Rare or Radiative Decays	26
LEPTON FLAVOR VIOLATION	27

*With permission from the Annual Review of Nuclear and Particle Science. Final version of this material is scheduled to appear in the Annual Review of Nuclear and Particle Science, Vol. 50, to be published in December 2000 by Annual Reviews (<http://www.AnnualReviews.org>)

$K_L^0 \rightarrow \mu e$	28
$K^+ \rightarrow \pi^+ \mu^+ e^-$	29
$K_L^0 \rightarrow \pi^0 \mu e$	29
<i>Other Searches for New Physics</i>	30
CONCLUSIONS AND FUTURE PROSPECTS 31	
<i>Medium-Rare and Radiative Decays</i>	31
$K \rightarrow \pi \nu \bar{\nu}$	32
EXPERIMENTAL CONFIGURATIONS 33	
<i>BNL: AGS</i>	33
<i>FNAL: Tevatron, Main Injector</i>	37
<i>NA48</i>	39
<i>KLOE</i>	40
<i>IHEP: Separated Kaon Experiment</i>	41
<i>KEK</i>	41
Acknowledgments	42

1 INTRODUCTION

This article reviews the status of rare kaon decays, with emphasis on the progress made since the 1993 review in this series [1]. Several other excellent review articles are available focusing on rare kaon decays [2], theoretical studies of rare kaon decays [3-6], and non-rare kaon decays [7]. Due to limited space, we cannot cover many interesting topics, such as CP violation in $K_L^0 \rightarrow \pi^+ \pi^-$ decays— ϵ and ϵ' , or T/CPT violation in $K_L^0 \rightarrow \pi^+ \pi^-$ decays, or searches for T violation in the transverse polarization of the μ^+ in $K^+ \rightarrow \pi^0 \mu^+ \nu_\mu \gamma$ and $K^+ \rightarrow \mu^+ \nu_\mu \gamma$.

Kaons have a relatively long lifetime because they decay only through the weak interaction. As a result, studies of their decays provide key insights into the behavior of the weak interaction under the three fundamental symmetry operators C , P , and T . The first of these, C or charge conjugation, is a unitary operator that replaces particles by anti-particles. Thus, in one possible sign convention, $C|K^0\rangle = -|\bar{K}^0\rangle$ and $C|K^+\rangle = -|\bar{K}^-\rangle$. The parity operator, P , inverts spatial directions, replacing left by right and vice-versa. The kaons are pseudoscalar particles which are odd under the action of P . Under the combined operator CP , then

$$\begin{aligned} CP|K^0\rangle &= |\bar{K}^0\rangle \\ CP|\bar{K}^0\rangle &= |K^0\rangle \end{aligned} \tag{1}$$

Even and odd eigenstates of CP called K_1 and K_2 can then be formed from the symmetric and antisymmetric combinations of the K^0 and \bar{K}^0 . If CP were an exact symmetry of the weak interaction, these combinations would be identified with the observed eigenstates of mass and lifetime, called K_S^0 and K_L^0 . The famous discovery in 1964 [8] of the decay $K_L^0 \rightarrow \pi\pi$ implied that CP symmetry is violated in weak decays, since the K_L , which decays mostly to CP -odd final states, can also decay to $\pi\pi$, which is CP -even. We have since learned that nearly all of the $K_L \rightarrow \pi\pi$ decay can be explained by so-called *indirect* CP violation, in which the mass and lifetime eigenstates K_L and K_S are mixtures of the CP eigenstates given by

$$|K_S^0\rangle = (|K_1\rangle + \epsilon|K_2\rangle) / \sqrt{1 + |\epsilon|^2} \tag{2}$$

$$|\bar{K}_L^0\rangle = (|K_2\rangle + \epsilon|K_1\rangle)/\sqrt{1+|\epsilon|^2},$$

and the decay proceeds via $\epsilon|K_1\rangle$. A question that has been open until recently is whether there is also *direct CP* violation, in which the *CP*-odd eigenstate K_2 decays to *CP*-even final states such as $\pi\pi$. The traditional method of searching for this phenomenon, which is expected in the Standard Model, is to look for a small deviation from unity of the so-called double ratio

$$R = \frac{\Gamma(K_L \rightarrow \pi^0\pi^0)/\Gamma(K_S \rightarrow \pi^0\pi^0)}{\Gamma(K_L \rightarrow \pi^+\pi^-)/\Gamma(K_S \rightarrow \pi^+\pi^-)}. \quad (3)$$

The value of this ratio has been reported [9,10] to be significantly different from unity, establishing the existence of direct *CP* violation in weak interactions. The Standard Model predicts a variety of other direct-*CP*-violating effects in rare kaon decays; measurements of these processes, which are addressed in this article, can provide additional tests of the Standard Model picture of *CP* violation.

The anti-unitary operator T reverses the arrow of time. In Lorentz-invariant local field theories, like the Standard Model, the combined operator *CPT* is an exact symmetry of the Lagrangian. Thus the observed *CP* violation in kaon decays would imply the existence of T violation. However, it is also interesting to search for more direct evidence of T violation, and a number of kaon-decay experiments have also played a central role in this effort.

The field of rare kaon decays has a long and rich history: the discovery of the kaon in 1949 [11], the postulation of “strangeness” [12], the τ - θ puzzle [13] and the understanding of parity violation [14], the understanding of quark mixing [15,16], the discovery of *CP* violation [8], the small rate for $K_L^0 \rightarrow \mu^+\mu^-$ and flavor-changing neutral currents (FCNCs) in general, and the development of the Glashow, Iliopoulos, Maiani (GIM) mechanism [17] and the prediction of the charm quark mass [18]. As the field has evolved, so has the definition of “rare” decays, from branching ratios of $\sim 10^{-3}$ to the current levels of $\sim 10^{-12}$.

This article will, in general, cover modes with branching ratios below $\sim 10^{-5}$, with one measured to be less than 10^{-11} . The two areas of greatest interest have been the very sensitive searches for physics beyond the standard model through lepton flavor-violating (LFV) decays and the studies of the standard-model picture of the Cabibbo, Kobayashi, Maskawa (CKM) mixing [16] and *CP* violation that have recently begun to bear fruit.

A large number of results from experiments at Brookhaven National Laboratory (BNL) (E787, E865, E871), Fermi National Accelerator Laboratory (FNAL) (E799-II: KTeV), and the European Laboratory for Particle Physics (CERN) (NA48) have been reported at recent conferences [19-31]. Many of these results have not yet been published.

1.1 Standard Model “Golden Modes” and CKM Matrix

The weak decay of quarks is described through the unitary CKM matrix. This matrix and the Wolfenstein parameterization [32,33] are shown below:

$$V_{\text{CKM}} = \begin{pmatrix} V_{ud} & V_{us} & V_{ub} \\ V_{cd} & V_{cs} & V_{cb} \\ V_{td} & V_{ts} & V_{tb} \end{pmatrix} \quad (4)$$

$$\begin{aligned} &\simeq \begin{pmatrix} 1 - \lambda^2/2 & \lambda & A\lambda^3(\rho - i\eta) \\ -\lambda & 1 - \lambda^2/2 & A\lambda^2 \\ A\lambda^3(1 - \rho - i\eta) & -A\lambda^2 & 1 \end{pmatrix} + \mathcal{O}(\lambda^4) \\ &\simeq \begin{pmatrix} 1 - \frac{\lambda^2}{2} - \frac{\lambda^4}{8} & \lambda & A\lambda^3(\rho - i\eta) \\ -\lambda + \frac{A^2\lambda^5(1-2\rho-2i\eta)}{2} & 1 - \frac{\lambda^2}{2} - \frac{\lambda^4}{8}(1+4A^2) & A\lambda^2 \\ A\lambda^3(1 - \bar{\rho} - i\bar{\eta}) & -A\lambda^2[1 - \lambda^2\frac{1-2\rho-i2\eta}{2}] & 1 - \frac{A^2\lambda^4}{2} \end{pmatrix}, \end{aligned}$$

where λ is the sin of the Cabibbo angle, $\lambda \equiv \sin \theta_C \simeq 0.22$, and $\bar{\rho}$ and $\bar{\eta}$ are related to the Wolfenstein parameters ρ and η by $\bar{\rho} \equiv \rho(1 - \lambda^2/2)$ and $\bar{\eta} \equiv \eta(1 - \lambda^2/2)$.

The unitarity of this matrix can be expressed in terms of six unitarity conditions which can be represented graphically in the form of triangles, all of which have the same area. The area of these triangles is equal to one half of the Jarlskog invariant, J_{CP} [34]. This is the fundamental measure of CP violation in the standard model. One of the possible unitarity relations that is frequently cited in the literature is

$$V_{ub}^* V_{ud} + V_{cb}^* V_{cd} + V_{tb}^* V_{td} = 0. \quad (5)$$

This equation can be represented graphically, as in Figure 1, where we have divided all sides by $V_{cb}^* V_{cd}$, which is a real quantity to $\mathcal{O}(\lambda^6)$. This particular

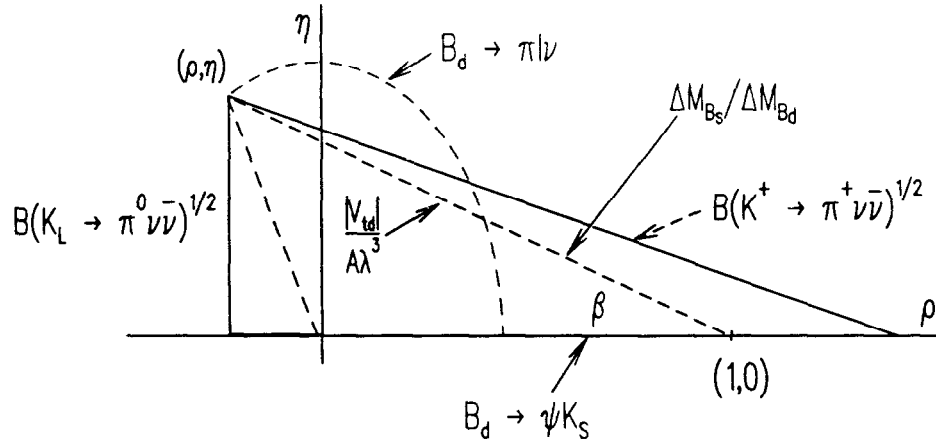


Figure 1: Traditional representation of the unitarity triangle. Measurements of B meson decays introduce constraints shown in green, contributions from the two golden kaon decay modes are marked in red.

representation provides a convenient display, with the apex of the triangle given by the two least well-known of the Wolfenstein parameters, $\bar{\rho}$ and $\bar{\eta}$. The best information currently comes from several measurements of B meson decays, as well as the measured value of ϵ from kaon decays. All of the unitarity triangles should be tested; it is desirable to overconstrain each of the unitarity relations and to measure J_{CP} in each of the triangles.

The most powerful tests of our understanding of CP -violation and quark mixing will come from comparison of the results from B meson and kaon decays with little theoretical ambiguity. The two premier tests are expected to be:

- Comparison of the angle β from the ratio $B(K_L^0 \rightarrow \pi^0 \nu \bar{\nu}) / B(K^+ \rightarrow \pi^+ \nu \bar{\nu})$ and the CP -violating asymmetry in the decay $B_d^0 \rightarrow \psi K_S^0$.

- Comparison of the magnitude $|V_{td}|$ from $K^+ \rightarrow \pi^+ \nu \bar{\nu}$ and the ratio of the mixing frequencies of B_s to B_d mesons, expressed in terms of the mass difference ratio $\Delta M_{B_s}/\Delta M_{B_d}$.

The current value of the fundamental level of CP violation in the SM, $J_{CP} = (2.7 \pm 1.1) \times 10^{-5}$, is known, primarily from measurements of B meson decays, with about 40% uncertainty [35]. Measurement of J_{CP} in the kaon system is very clean theoretically (uncertainty of $\sim 2\%$) and can be expected to be measured to $\sim 8\%$ within a decade. While measurement of J_{CP} in the B system is difficult and is plagued by theoretical uncertainties, it is likely that a 15% measurement is possible and if this could be pushed to the level expected from the kaon system, the comparison of these values will also be an important test of the SM.

1.2 Form Factor Measurements

Interest in rare kaon decays extends well beyond their potential to determine standard-model parameters. Dozens of different medium-rare (branching ratios in the range 10^{-5} to 10^{-8}) kaon decays have been measured. With the ever-increasing sensitivity of experiments designed to search for the very-rare modes that probe standard-model parameters or search for new physics, the statistics available for these medium-rare decays have increased to the point where both precision branching ratio measurements and form factor studies are possible.

Both the branching ratios and the form factors provide excellent tests of chiral perturbation theory (ChPT) [36,37], which should work well at the relatively low momentum scales characteristic of kaon decays. The wide variety of different modes and form factors can be used to test ChPT.

Measurements of a number of modes, such as $K_L^0 \rightarrow e^+ e^- \gamma \gamma$ and $K_L^0 \rightarrow \pi^0 \gamma \gamma$, are directly relevant to the determination of standard-model parameters because these modes can be backgrounds to more interesting decays, such as $K_L^0 \rightarrow \pi^0 e^+ e^-$ or $K_L^0 \rightarrow \pi^0 \nu \bar{\nu}$. They can also provide information necessary to disentangle different amplitudes contributing to the signal mode, such as the $\pi^0 \gamma^* \gamma^*$ intermediate state for $K_L^0 \rightarrow \pi^0 e^+ e^-$ or the $\gamma^* \gamma^*$ intermediate state for $K_L^0 \rightarrow \mu^+ \mu^-$.

The study of these “non-marquee” decay modes is thus more than a beneficial by-product of experiments designed to search for the more significant decays. Their properties are often of vital importance to the determination of backgrounds, the extraction of standard-model parameters, or tests of the reliability of theoretical tools like ChPT.

1.3 Searches for New Physics

A major thread in the history of the study of rare kaon decays is the search for exotic phenomena, often referred to as “beyond the standard model” (BSM). The quintessential example is the long search for the decay $K_L^0 \rightarrow \mu e$. This decay is absolutely forbidden in the standard model with massless neutrinos; specifically, it is forbidden by the symmetry of conserved lepton flavor number, for which no fundamental reason is known. Grand unified theories or other extensions to the standard model often contain heavy vector bosons that connect the standard-model lepton families—for example, coupling muons to electrons (horizontal gauge bosons) or quarks to leptons (leptoquarks). Both types of particles could mediate the otherwise forbidden decays, such as $K_L^0 \rightarrow \mu e$ or $K \rightarrow \pi \mu e$.

Because these decays simply do not happen in the standard model and are relatively simple to detect, they provide exceptional sensitivity to BSM physics. With experiments now probing branching ratios at the level of 10^{-12} , even a very heavy exotic boson (on the order of 100 TeV, for the usual electroweak coupling) would lead to a detectable signal.

2 CP VIOLATION AND THE CKM MATRIX

The unitarity triangle is most readily expressed for the kaon system as follows:

$$V_{us}^* V_{ud} + V_{cs}^* V_{cd} + V_{ts}^* V_{td} = 0 \quad (6)$$

or

$$\lambda_u + \lambda_c + \lambda_t = 0,$$

with the three vectors $\lambda_i \equiv V_{is}^* V_{id}$ converging to form a very elongated triangle in the complex plane. This is illustrated graphically in Figure 2. The first vector,

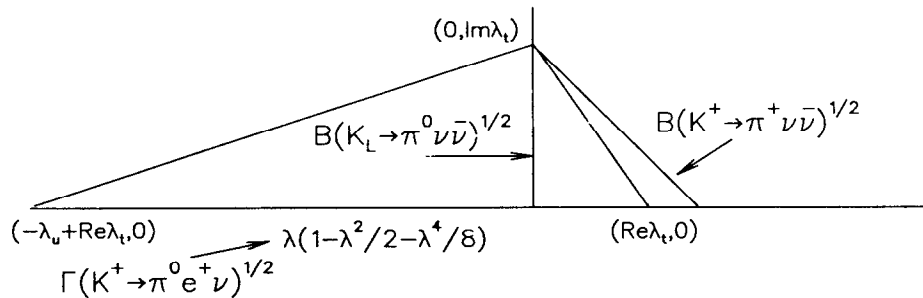


Figure 2: Unitarity triangle for the K system (not to scale).

$\lambda_u = V_{us}^* V_{ud}$, is well known. The height will be measured by $K_L^0 \rightarrow \pi^0 \nu \bar{\nu}$ and the third vector, $\lambda_t = V_{ts}^* V_{td}$, will be measured by the decay $K^+ \rightarrow \pi^+ \nu \bar{\nu}$. The theoretical ambiguities in interpreting all of these measurements are very small. It may be possible to extract additional constraints on the height of the triangle from $K_L^0 \rightarrow \pi^0 \ell^+ \ell^-$ decays and on $\text{Re}(\lambda_t)$ from $K_L^0 \rightarrow \mu^+ \mu^-$ decays.

The base of this triangle has the length $b \equiv \lambda_u = V_{us}^* V_{ud}$, determined from the decay rate of $K \rightarrow \pi e \nu_e$ and nuclear beta decay. If we assume unitarity then b is determined completely from $K \rightarrow \pi e \nu_e$ and $b = |V_{us}|$ to very good approximation. To even better accuracy it is expressed as

$$b = \lambda - \frac{\lambda^3}{2} - \frac{\lambda^5}{8}. \quad (7)$$

The value of λ , the best-known of the Wolfenstein parameters, is extracted [38] from the measurement of the $K \rightarrow \pi e \nu_e$ rate [39]. The height of the triangle, $h \equiv \text{Im}(\lambda_t)$ can be derived from a measurement of the $K_L^0 \rightarrow \pi^0 \nu \bar{\nu}$ branching ratio. The area of the triangle, a , is then given by two kaon decay measurements as

$$J_{CP} = 2a = b \times h = \lambda_u \times \text{Im}(\lambda_t) = 0.976 \times \lambda \times \text{Im}(\lambda_t); \quad (8)$$

the ultimate uncertainty on $\text{Im}(\lambda_t)$ and a will be limited, not by theoretical ambiguities, but by experimental uncertainties on $B(K_L^0 \rightarrow \pi^0 \nu \bar{\nu})$, to $\mathcal{O}(5-10\%)$ from the next round of $K_L^0 \rightarrow \pi^0 \nu \bar{\nu}$ experiments. This compares favorably to the

B system, where three (four without the unitarity assumption) measurements are needed.

Table 1 lists current values [39-41] for the magnitudes of the CKM matrix elements and Wolfenstein parameters.

Table 1: Magnitudes of CKM matrix parameters. The current values for the matrix elements V_{ji} are listed, where i loops over the d -type and j represents the u -type quarks, as are the $\lambda_j \equiv V_{js}^* V_{jd}$ values as defined earlier in the text and the Wolfenstein parameters (λ , A , ρ and η).

V_{ji}	i=d	i=s	i=b	$\lambda_j \equiv V_{js}^* V_{jd}$
V_{ui}	0.9740 ± 0.0010	0.2196 ± 0.0023	0.0032 ± 0.0008	0.2139 ± 0.0026
V_{ci}	0.224 ± 0.016	1.04 ± 0.16	0.0395 ± 0.0017	0.233 ± 0.040
V_{ti}	0.0084 ± 0.0018^1	$\sim V_{cb}^{-1}$	0.99 ± 0.29	$.00033 \pm .00009$
λ	0.2196 ± 0.0023 [39]			
A	0.819 ± 0.039 [39]			
ρ	0.14 ± 0.15 [40]		$(0.18 \pm 0.04$ [41]) ²	
η	0.38 ± 0.13 [40]		$(0.36 \pm 0.03$ [41]) ²	

^aThe entries for V_{td} and V_{ts} assume a 3 generation unitary matrix.

^bThe uncertainties on ρ and η are conservative, generally accepted values. Values from more aggressive treatment of errors are given in parentheses.

2.1 $K_L^0 \rightarrow \mu^+ \mu^-$

The decay $K_L^0 \rightarrow \mu^+ \mu^-$ is dominated by the process of $K_L^0 \rightarrow \gamma\gamma$ with the two real photons converting to a $\mu^+ \mu^-$ pair. This contribution can be precisely calculated in QED [42] based on a measurement of the $K_L^0 \rightarrow \gamma\gamma$ branching ratio. However, there is also a long-distance dispersive contribution, through off-shell photons. This contribution needs additional input from ChPT [43,44], which may be aided by new, improved measurements of the decays $K_L^0 \rightarrow e^+ e^- \gamma$, $K_L^0 \rightarrow \mu^+ \mu^- \gamma$, $K_L^0 \rightarrow e^+ e^- e^+ e^-$ and $K_L^0 \rightarrow \mu^+ \mu^- e^+ e^-$ (see Section 3.1), although there is some dispute as to the reliability of such calculations [45,46]. Most interesting is the short-distance contribution which proceeds through internal quark loops, dominated by the top quark (see Figure 3). This contribution is sensitive to

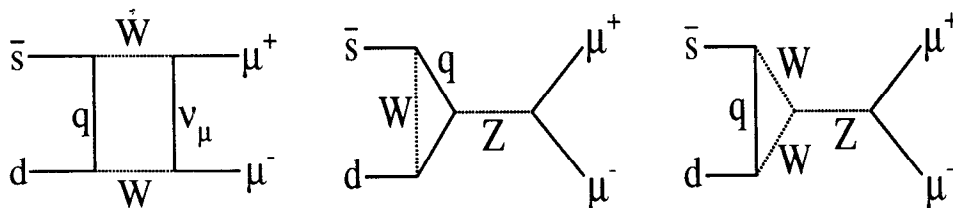


Figure 3: Feynman diagrams for the short-distance component of the decay $K_L^0 \rightarrow \mu^+ \mu^-$.

the real part of the poorly known CKM matrix element V_{td} or equivalently to ρ [5,47]. If this were the only contribution to the decay, the branching ratio

$B_{SD}(K_L^0 \rightarrow \mu^+ \mu^-)$ could be written as

$$\begin{aligned} B_{SD}(K_L^0 \rightarrow \mu^+ \mu^-) &= \frac{\tau_L}{\tau_{K^+}} \frac{\alpha^2 B(K_{\mu 2})}{\pi^2 \sin^4 \theta_W |V_{us}|^2} [Y_c \text{Re}(\lambda_c) + Y_t \text{Re}(\lambda_t)]^2 \quad (9) \\ &= 1.51 \times 10^{-9} A^4 (\rho_0 - \bar{\rho})^2, \end{aligned}$$

with $\rho_0 = 1.2$ and the Inami-Lim functions [5,48], Y_q , are functions of $x_q \equiv M_q^2/M_W^2$ where M_W is the mass of the W boson and M_q is the mass of the quark q . This mode has now been measured with impressively high statistics [49] (see Figure 4) by the E871 collaboration (see Section 6.1.2). The branching ratio,

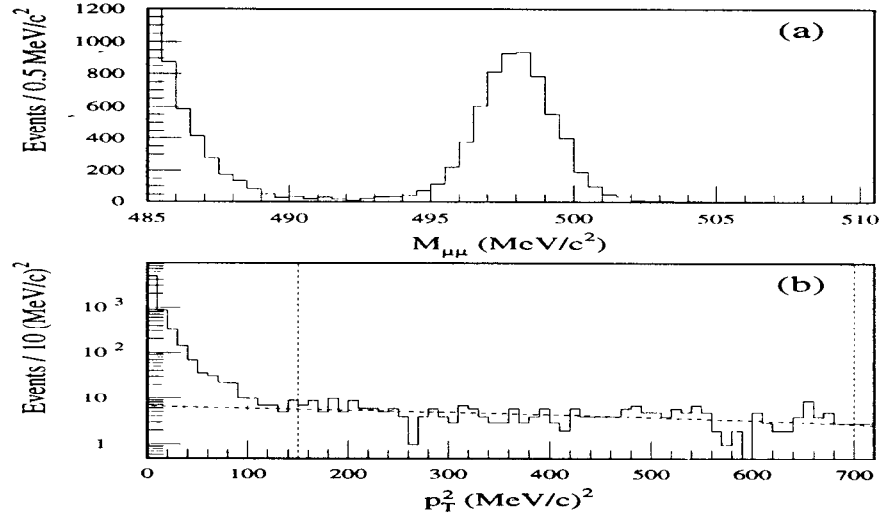


Figure 4: Final sample of $K_L^0 \rightarrow \mu^+ \mu^-$ decays from experiment E871 at BNL. A total of ~ 6200 $K_L^0 \rightarrow \mu^+ \mu^-$ events are observed in the peak. a) Reconstructed mass of the $\mu^+ \mu^-$ pair, $M_{\mu\mu}$ and b) the momentum of the reconstructed $\mu^+ \mu^-$ pair relative to that of the parent kaon (p_T), where the direction of the parent kaon is derived from the locations of the target and the decay vertex.

$B(K_L^0 \rightarrow \mu^+ \mu^-) = (7.18 \pm 0.17) \times 10^{-9}$, is a factor of three more precise than previous measurements, and the error on the rate relative to $K_L^0 \rightarrow \pi^+ \pi^-$,

$$\frac{\Gamma(K_L^0 \rightarrow \mu^+ \mu^-)}{\Gamma(K_L^0 \rightarrow \pi^+ \pi^-)} = (3.474 \pm 0.054) \times 10^{-6}, \quad (10)$$

no longer dominates the error on the ratio

$$\frac{\Gamma(K_L^0 \rightarrow \mu^+ \mu^-)}{\Gamma(K_L^0 \rightarrow \gamma\gamma)} = (1.213 \pm 0.030) \times 10^{-5}, \quad (11)$$

contributing only $\sim 1.5\%$ of the 2.5% error. The remaining significant sources of uncertainty,

$$\frac{\Gamma(K_L^0 \rightarrow \gamma\gamma)}{\Gamma(K_L^0 \rightarrow \pi^0 \pi^0)} = 0.632 \pm 0.009, \quad \frac{\Gamma(K_S^0 \rightarrow \pi^+ \pi^-)}{\Gamma(K_S^0 \rightarrow \pi^0 \pi^0)} = 2.186 \pm 0.028, \quad (12)$$

will probably be improved in the near future by the KLOE experiment at Frascati.

This measured ratio is only slightly above the unitarity bound from the on-shell two-photon contribution

$$\frac{\Gamma(K_L^0 \rightarrow \mu^+ \mu^-)}{\Gamma(K_L^0 \rightarrow \gamma\gamma)} = 1.195 \times 10^{-5} \quad (13)$$

and limits possible short-distance contributions. With a recent estimate of the long-distance dispersive contribution [43], a limit on ρ was extracted: $\rho > -0.33$ at 90% confidence level (CL) [49].

Unlike $K_L^0 \rightarrow \mu^+ \mu^-$, which is predominantly mediated by two real photons, the decay $K_L^0 \rightarrow e^+ e^-$ proceeds primarily via two off-shell photons. The relative contribution from short-distance top loops is significantly smaller than in $K_L^0 \rightarrow \mu^+ \mu^-$. However, the recent observation by E871 [50] of four events, with a branching ratio of $B(K_L^0 \rightarrow e^+ e^-) = (8.7_{-4.1}^{+5.7}) \times 10^{-12}$, is consistent with ChPT predictions [44,45] and is the smallest branching ratio ever measured for any elementary particle decay.

2.2 $K_L^0 \rightarrow \pi^0 \ell^+ \ell^-$

The decays $K_L^0 \rightarrow \pi^0 e^+ e^-$ and $K_L^0 \rightarrow \pi^0 \mu^+ \mu^-$ can proceed via the direct- CP -violating components of the diagrams in Figure 3 and the $s \rightarrow d\gamma^*$ amplitude, where γ^* represents a virtual photon. These processes are calculable with high precision within the Standard Model since they are dominated by top-quark exchange. If these were the only contributions to this decay, the branching ratio for $K_L^0 \rightarrow \pi^0 e^+ e^-$ would be related to the CKM matrix elements by [51]

$$\begin{aligned} B_{SD}(K_L^0 \rightarrow \pi^0 e^+ e^-) &= \frac{\tau_L \alpha^2 B(K_{e3})}{\tau_K + 4\pi^2 |V_{us}|^2} (y_{7A}^2 + y_{7V}^2) |Im(\lambda_t)|^2 \\ &= 6.91 \times 10^{-11} A^4 \eta^2, \end{aligned} \quad (14)$$

With the current best-fit value of 1.38×10^{-4} for $Im(\lambda_t)$ [52], this implies a branching ratio of about 5×10^{-12} . The related decay $K_L^0 \rightarrow \pi^0 \mu^+ \mu^-$ is expected to be suppressed relative to the electron mode by about a factor of five owing to the reduced phase space.

Unfortunately, the decay $K_L^0 \rightarrow \pi^0 e^+ e^-$ can occur in two other ways. First, there is an indirect- CP -violating contribution from the CP -even, K_1^0 component of K_L^0 . This contribution could be determined from a measurement of $K_S^0 \rightarrow \pi^0 e^+ e^-$, but the current upper limit [53] of $B(K_S^0 \rightarrow \pi^0 e^+ e^-) < 1.1 \times 10^{-6}$ is far from the expected level of less than 10^{-8} . A K_S branching ratio of 10^{-9} would imply an indirect- CP -violating contribution to $K_L^0 \rightarrow \pi^0 e^+ e^-$ of about 3×10^{-12} , comparable to the expected direct- CP -violating contribution. In addition, a significant contribution is expected from the interference between the direct and indirect- CP -violating amplitudes.

Further complicating the picture is the presence of a CP -conserving amplitude involving a $\pi^0 \gamma^* \gamma^*$ intermediate state, from which the virtual photons materialize into an $e^+ e^-$ pair. A model for the $K_L^0 \pi^0 \gamma^* \gamma^*$ vertex is needed to determine the size of this contribution. This vertex can be studied by measuring the $K_L^0 \rightarrow \pi^0 \gamma\gamma$ decay and the related decay $K_L^0 \rightarrow \pi^0 e^+ e^- \gamma$. These decays are discussed in Section 3.2. Based on recent measurements of these modes, by the KTeV experiment at Fermilab (see Section 6.2.1), the CP -conserving contribution to $K_L^0 \rightarrow \pi^0 e^+ e^-$ has been estimated at $1-2 \times 10^{-12}$, comparable to the expected direct- CP -violating part.

Given these three contributions, it will be difficult to extract CKM matrix parameters from even a precision measurement of $K_L^0 \rightarrow \pi^0 e^+ e^-$. But there is a still more formidable roadblock to progress on these modes, first pointed out by Greenlee [54]. As is discussed in Section 3.1, the radiative Dalitz decay $K_L^0 \rightarrow e^+ e^- \gamma \gamma$ has a rather large branching ratio ($\sim 6 \times 10^{-7}$). The two photons may have an invariant mass near that of the π^0 , so that the final state is indistinguishable from the $\pi^0 e^+ e^-$ mode. Two strategies can be used to deal with this background. First, a high-precision calorimeter can be used to minimize the size of the region in $M_{\gamma\gamma}$ where confusion can occur; second, the difference in the kinematic distributions expected in the radiative Dalitz decay can be used to remove most of the background events, at a cost of some acceptance for the signal mode $K_L^0 \rightarrow \pi^0 e^+ e^-$. These techniques reduce, but cannot eliminate, this background, so that the present searches for $K_L^0 \rightarrow \pi^0 e^+ e^-$ are background-limited at the level of 10^{-10} .

The most recent limit on $K_L^0 \rightarrow \pi^0 e^+ e^-$ comes from the KTeV experiment [55]. The analysis selects on the direction of the photons with respect to the electrons to minimize the background from radiative Dalitz decays while preserving as much sensitivity as possible. Figure 5a shows the $ee\gamma\gamma$ mass vs the $\gamma\gamma$ mass for the KTeV data with the signal box excluded, and Figure 5b shows an expanded view around the signal box. KTeV found two events that passed all cuts, compared

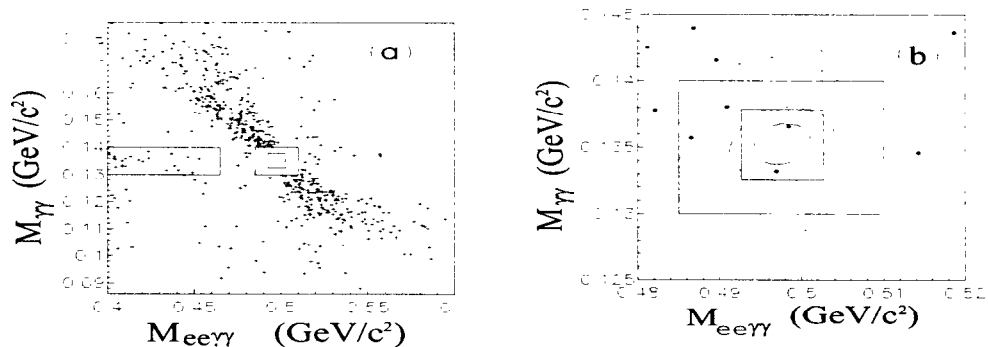


Figure 5: KTeV: Reconstructed $\pi^0 e^+ e^-$ mass plotted vs reconstructed $\gamma\gamma$ mass from the $K_L^0 \rightarrow \pi^0 e^+ e^-$ analysis of 1996-1997 data. a) shows the situation before the final set of kinematic cuts, and the diagonal band passing through the signal region is due to the background mode $K_L^0 \rightarrow e^+ e^- \gamma \gamma$. Events in the exclusion box surrounding the signal box are not shown. b) shows the two events remaining in the signal region (the smallest box) after all cuts are applied. The contours contain 68% and 95% of any real $K_L^0 \rightarrow \pi^0 e^+ e^-$ signal.

with an expected background level of 1.06 events. This finding leads to an upper limit $B(K_L^0 \rightarrow \pi^0 e^+ e^-) < 5.6 \times 10^{-10}$ (90% CL). Although this limit represents a significant improvement over previous results [56-58], it is still two orders of magnitude above the standard-model prediction for the direct- CP -violating component of this decay.

A similar analysis of the related muon mode by KTeV resulted in a slightly

smaller upper limit [59], $B(K_L^0 \rightarrow \pi^0 \mu^+ \mu^-) < 3.4 \times 10^{-10}$ (90% CL). Figure 6 shows a plot of the $\pi^0 \mu \mu$ mass, with two events in the signal region and an

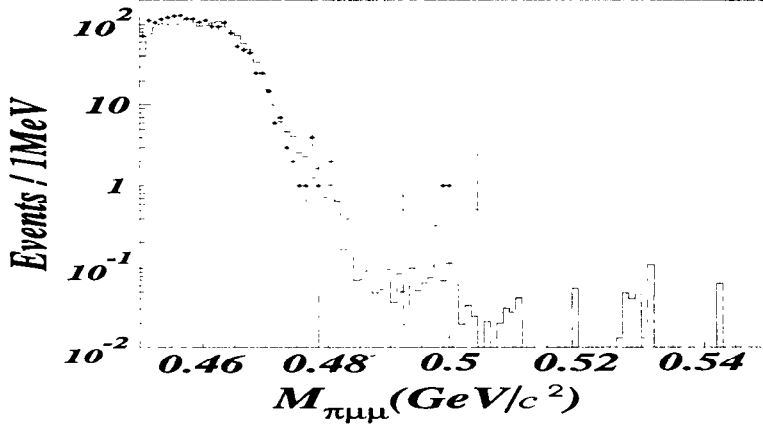


Figure 6: KTeV: Invariant mass distribution, $M_{\pi^0 \mu \mu}$, for events passing all other cuts from the 1996-1997 data set.

expected background of 0.87 ± 0.15 . The greater sensitivity for this mode results from making looser kinematic cuts. Due to the reduced phase space for this decay, the branching ratio of the muon mode is expected to be a factor of five smaller than that for the electron mode, so that this limit is farther from the expected level than the limit for $\pi^0 e^+ e^-$. An improvement of roughly a factor of two may be expected in both these limits when the analysis of the 1999 KTeV data set is complete.

Table 2 summarizes the experimental measurements of $K^0 \rightarrow \pi^0 \ell^+ \ell^-$. The ob-

Table 2: Summary of $K^0 \rightarrow \pi^0 \ell^+ \ell^-$ results

Decay Mode	Branching Ratio	Experiment
$K_L^0 \rightarrow \pi^0 e^+ e^-$	$< 5.6 \times 10^{-10}$	KTeV (1999) [55]
$K_L^0 \rightarrow \pi^0 \mu^+ \mu^-$	$< 3.4 \times 10^{-10}$	KTeV (2000) [59]
$K_S^0 \rightarrow \pi^0 e^+ e^-$	$< 1.1 \times 10^{-6}$	NA31 (1993) [53]

stacles to determining CKM matrix elements from measurements of the $K_L^0 \rightarrow \pi^0 \ell^+ \ell^-$ modes are formidable. Although work on these modes is likely to continue, future efforts will focus on the related decay $K_L^0 \rightarrow \pi^0 \nu \bar{\nu}$, which is free of the problems affecting the $\pi^0 e^+ e^-$ and $\pi^0 \mu^+ \mu^-$ modes.

2.3 $K \rightarrow \pi \nu \bar{\nu}$

The decay modes $K^+ \rightarrow \pi^+ \nu \bar{\nu}$ and $K_L^0 \rightarrow \pi^0 \nu \bar{\nu}$ are the golden modes for determining the CKM parameters ρ and η . Together with the other golden mode $B_d^0 \rightarrow \psi K_S^0$, and perhaps the ratio $\Delta M_{B_s} / \Delta M_{B_d}$, they provide the best opportunity to test the Standard Model explanation of CP violation and to search for new physics. The $K \rightarrow \pi \nu \bar{\nu}$ decays are sensitive to the magnitude and imaginary part of V_{td} . From these two modes, the unitarity triangle can be completely determined.

These modes proceed through loops dominated by the top quark, as shown in Figure 7. The hadronic matrix element for these decays can be extracted from

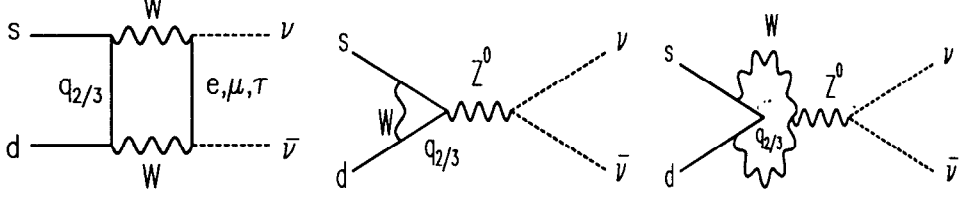


Figure 7: Feynman diagrams for the decays $K \rightarrow \pi \nu \bar{\nu}$.

the well-measured $K^+ \rightarrow \pi^0 e^+ \nu_e$ (K_{e3}) decay. The branching ratios have been calculated in the next-to-leading-log approximation [60], complete with corrections for isospin violation [61] and two-loop-electroweak effects [62]. They can be expressed as follows [63]:

$$B(K_L^0 \rightarrow \pi^0 \nu \bar{\nu}) = \frac{\tau_L}{\tau_K} \frac{\kappa_L \alpha^2 B(K_{e3})}{2\pi^2 \sin^4 \theta_W |V_{us}|^2} \sum_l |Im(\lambda_t) X_t|^2 \quad (15)$$

$$B(K^+ \rightarrow \pi^+ \nu \bar{\nu}) = \frac{\kappa_+ \alpha^2 B(K_{e3})}{2\pi^2 \sin^4 \theta_W |V_{us}|^2} \sum_l |X_t \lambda_t + X_c \lambda_c|^2.$$

The factors κ_L and κ_+ refer to the isospin corrections relating $K \rightarrow \pi \nu \bar{\nu}$ to $K^+ \rightarrow \pi^0 e^+ \nu_e$. The Inami-Lim functions [5,48], X_q , are also functions of x_q ; these contain QCD corrections. The sum is over the three neutrino generations. (See Reference 63 for more information). The intrinsic theoretical uncertainty in the branching ratio $B(K^+ \rightarrow \pi^+ \nu \bar{\nu})$ is 7%, predominantly from the next-to-leading-log calculation of X_c . The intrinsic theoretical uncertainty for $K_L^0 \rightarrow \pi^0 \nu \bar{\nu}$ is even smaller, $\sim 2\%$, coming from the uncertainties in κ_L and X . These equations can be rewritten in terms of the Wolfenstein parameters, and based on our current understanding of standard-model parameters, the branching ratios are predicted to be

$$B(K_L^0 \rightarrow \pi^0 \nu \bar{\nu}) = 4.08 \times 10^{-10} A^4 \eta^2 \quad (16)$$

$$= (3.1 \pm 1.3) \times 10^{-11}$$

$$B(K^+ \rightarrow \pi^+ \nu \bar{\nu}) = 8.88 \times 10^{-11} A^4 [(\bar{\rho}_0 - \bar{\rho})^2 + (\sigma \bar{\eta})^2] \quad (17)$$

$$= (8.2 \pm 3.2) \times 10^{-11},$$

where $\sigma = (1 - \frac{\lambda^2}{2})^{-2}$ and $\bar{\rho}_0 = 1.4$ [63]. In addition, it is possible to place a theoretically unambiguous upper limit on $K^+ \rightarrow \pi^+ \nu \bar{\nu}$ from the limit on $\Delta M_{B_s} / \Delta M_{B_d}$ derived from $\Delta M_{B_s} < 14.3 \text{ ps}^{-1}$ [64]. This limit is [63]

$$B(K^+ \rightarrow \pi^+ \nu \bar{\nu}) < 1.67 \times 10^{-10}. \quad (18)$$

The decay amplitude $K_L^0 \rightarrow \pi^0 \nu \bar{\nu}$ is direct- CP -violating, and offers the best opportunity for measuring the Jarlskog invariant J_{CP} . Although the B meson system will provide clean measures of some angles of the triangle, the determination of its area will be much less precise.

Two sets of recent experimental results have stimulated a lot of theoretical activity on various BSM contributions [52,65] to $K \rightarrow \pi \nu \bar{\nu}$. The value of $Re(\epsilon'/\epsilon) = (19.3 \pm 2.4) \times 10^{-4}$, including the most recent experimental results [9,10], is larger

than most theoretical calculations have predicted [3,5,52,66]. In addition, the first observation of $K^+ \rightarrow \pi^+ \nu \bar{\nu}$ from E787 based data collected in 1995 [67], with $B(K^+ \rightarrow \pi^+ \nu \bar{\nu}) = 4.2_{-3.5}^{+9.7} \times 10^{-10}$, was a factor of five larger than the standard-model prediction. The theoretical calculation of ϵ'/ϵ has large uncertainty, so although the measured value is higher than most calculations, this does not necessarily imply the need for new physics. The same is true of the $K^+ \rightarrow \pi^+ \nu \bar{\nu}$ measurement; although the standard-model prediction is unambiguous and the result was high, the branching ratio based on one event is entirely consistent with the standard model. Reference 65 points out that in a generic supersymmetric extension to the standard model, an enhanced Zds or sdg vertex that contributes to ϵ'/ϵ will also enhance either $K_L^0 \rightarrow \pi^0 \nu \bar{\nu}$ or $K_L^0 \rightarrow \pi^0 e^+ e^-$. The enhancement of $K^+ \rightarrow \pi^+ \nu \bar{\nu}$ is smaller, as it is limited to some extent by the measured value of $K_L^0 \rightarrow \mu^+ \mu^-$. An enhancement in these rare modes would be much easier to interpret than in ϵ'/ϵ .

2.3.1 $K^+ \rightarrow \pi^+ \nu \bar{\nu}$

Although the decay $K^+ \rightarrow \pi^+ \nu \bar{\nu}$ is attractive theoretically, it is quite challenging experimentally. Not only is the branching ratio expected to be less than 10^{-10} , it is a three-body decay with two undetectable neutrinos. The key to a convincing measurement of this decay is a thorough understanding of the background at a level of 10^{-11} . The E787 experiment (see Section 6.1.3) previously reported results of the analysis of the 1995 data sample [67]. This experiment employs two guiding principles for determining the background:

- The background is measured from the same data as the $K^+ \rightarrow \pi^+ \nu \bar{\nu}$ signal. In this manner, any hardware problems, changes in rates, or changes in detector performance are automatically considered.
- For all background from kaon decays, two independent sets of selection criteria are devised, with large rejection (e.g. typical rejections are $R > 100$) for that background type. This allows a measurement of background levels at a sensitivity R times greater than the signal by reversing one set of selection criteria. Because one set of criteria is always reversed, the criteria are devised without any bias from examining events in the signal region.

The three major sources of background, $K^+ \rightarrow \mu^+ \nu_\mu$, $K^+ \rightarrow \pi^+ \pi^0$, and pions from the beam, are all measured, with a total background of 0.08 ± 0.02 events from the analysis of the data collected during 1995–1997. One clean $K^+ \rightarrow \pi^+ \nu \bar{\nu}$ event was found (see Figure 8), and based on this one event [68], which was also seen in the earlier data, the branching ratio is $B(K^+ \rightarrow \pi^+ \nu \bar{\nu}) = 1.5_{-1.2}^{+3.4} \times 10^{-10}$. This measurement places a limit on $|V_{td}|$ —and without any reference to measurements from B meson decays, limits on λ_t can be derived:

$$\begin{aligned}
 0.002 < |V_{td}| < 0.04 & \quad (19) \\
 |Im(\lambda_t)| < 1.22 \times 10^{-3} \\
 -1.10 \times 10^{-3} < Re(\lambda_t) < 1.39 \times 10^{-3} \\
 1.07 \times 10^{-4} < |\lambda_t| < 1.39 \times 10^{-3}.
 \end{aligned}$$

The E787 experiment, with all data recorded should reach a factor of two higher sensitivity—to the level of the standard-model expectation for $K^+ \rightarrow \pi^+ \nu \bar{\nu}$.

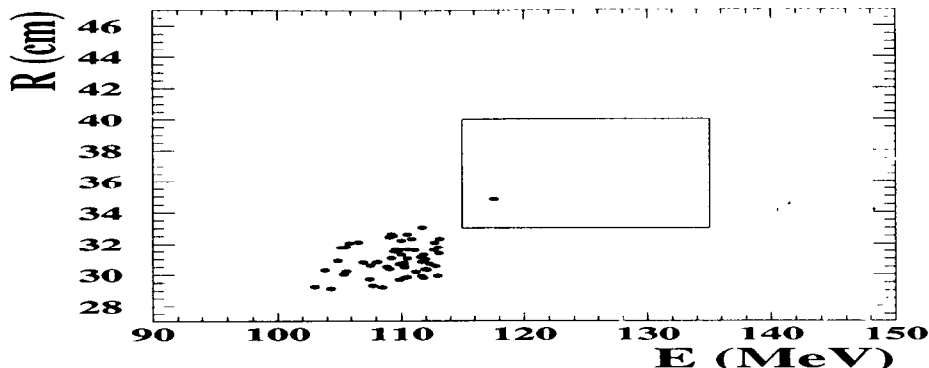


Figure 8: E787: Final data sample collected in 1995–1997 after all cuts. One clean $K^+ \rightarrow \pi^+ \nu \bar{\nu}$ event is seen in the signal box. The remaining events are $K^+ \rightarrow \pi^+ \pi^0$ background.

A new experiment, E949 (see Section 6.1.3), is under construction at BNL and will run from 2001 through 2003. Taking advantage of the large AGS proton flux and the experience gained with the E787 detector, E949 should observe 10 standard-model events in a two-year run. The background is well understood and based on E787 measurements is expected to be 10% of the standard-model signal. A proposal for an experiment which promises a further factor of 10 improvement has been prepared at FNAL. The CKM experiment (E905) is designed to collect 100 standard-model events, with an estimated background of approximately 10% of the signal, in a two-year run starting in about 2005. This experiment will use a new technique, with K^+ decay-in-flight and momentum/velocity spectrometers.

2.3.2 $K_L^0 \rightarrow \pi^0 \nu \bar{\nu}$

The decay $K_L^0 \rightarrow \pi^0 \nu \bar{\nu}$ is even cleaner theoretically and is purely direct- CP -violating. Unfortunately, it is even more difficult experimentally, because all particles involved in the initial and final states are neutral.

Presently, the best limit on $K_L^0 \rightarrow \pi^0 \nu \bar{\nu}$ is derived in a model-independent way [69] from the E787 measurement of $K^+ \rightarrow \pi^+ \nu \bar{\nu}$:

$$\begin{aligned} B(K_L^0 \rightarrow \pi^0 \nu \bar{\nu}) &< 4.4 \times B(K^+ \rightarrow \pi^+ \nu \bar{\nu}) \\ &< 2.6 \times 10^{-9} \text{ (90\% CL)}. \end{aligned} \quad (20)$$

The goal is to observe this mode directly in order to extract a second of the CKM matrix parameters. Here we concentrate on the high-transverse-momentum technique for making this measurement, as used in the existing KTeV results; future efforts toward measuring $K_L^0 \rightarrow \pi^0 \nu \bar{\nu}$ may also include center-of-mass experiments. The $K_L^0 \rightarrow \pi^0 \nu \bar{\nu}$ decay is identified by two photons from the common decay $\pi^0 \rightarrow \gamma\gamma$. K_L decays such as $K_L^0 \rightarrow \pi^0 \pi^0 \pi^0$ and $K_L^0 \rightarrow \pi^0 \pi^0$ can easily produce background if all but two of the final-state photons are unobserved. Background can also arise from π^0 's produced by Λ or Ξ^0 hyperon decays to final states such as $n\pi^0$ with the neutron undetected, if the beam contains large numbers of hyperons. An excellent system of photon veto detectors can substantially reduce these backgrounds, but additional kinematic cuts will also be necessary. In the center of mass experiments, a simple invariant mass cut can be made to reject

$K_L^0 \rightarrow \pi^0 \pi^0$ and $K_L^0 \rightarrow \pi^0 \pi^0 \pi^0$ backgrounds. In experiments like KTeV where the kaon momentum is unknown, one can exploit the fact that the neutrinos recoiling against the π^0 in $K_L^0 \rightarrow \pi^0 \nu \bar{\nu}$ are massless, so that the transverse momentum of the π^0 extends to larger values than are possible in the background modes, as shown in Figure 9.

KTeV (see Section 6.2.1) does not measure the kaon momentum; in order to determine the transverse momentum of the π^0 , the decay vertex must be known. The longitudinal position of the vertex can be determined from the invariant mass constraint, but the transverse position can only be known within the size of the kaon beam. Thus a narrow ‘‘pencil’’ beam is needed, which limits the available intensity. KTeV tried this approach in a one-day test run and observed one background event, probably from a neutron interaction. From this special run, a 90%-CL limit [70] of $B(K_L^0 \rightarrow \pi^0 \nu \bar{\nu}) < 1.6 \times 10^{-6}$ was determined. An alternative is to use the rarer $\pi^0 \rightarrow e^+ e^- \gamma$ decay. This is a factor of 80 less sensitive but has several advantages. First, the location of the decay vertex can be determined from the charged tracks, so that a high-intensity, wide neutral beam can be used. This allowed the KTeV data for this mode to be taken in the standard configuration with standard triggers. Second, this approach allows determination of the transverse momentum with better precision, reducing the background level. The P_T distribution of π^0 events passing all other cuts can be seen in Figure 9. The backgrounds nearest the search region come from the

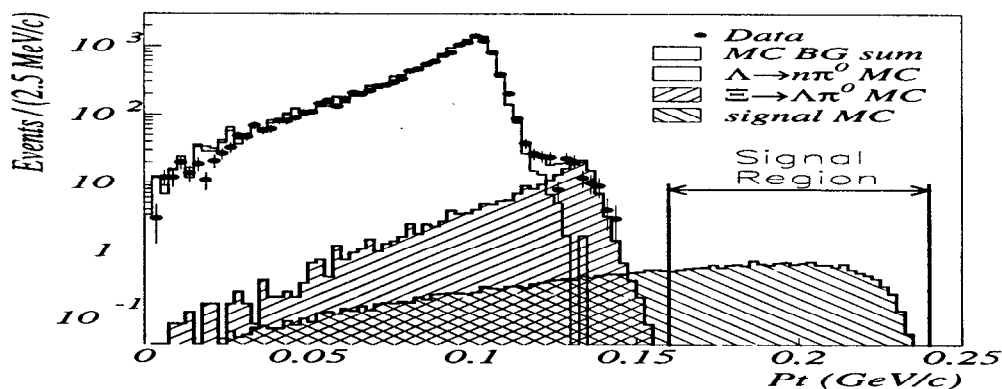


Figure 9: KTeV: Final $K_L^0 \rightarrow \pi^0 \nu \bar{\nu}$ data sample collected during 1996–1997 after all cuts. No $K_L^0 \rightarrow \pi^0 \nu \bar{\nu}$ events are seen above $P_T = 160$ MeV/c.

decays $\Lambda \rightarrow n \pi^0$ and $\Xi^0 \rightarrow \Lambda \pi^0$. In this search using the full 1997 KTeV data set, with an expected background of $0.12^{+0.05}_{-0.04}$, no events were seen, and at the 90% confidence level, $B(K_L^0 \rightarrow \pi^0 \nu \bar{\nu}) < 5.9 \times 10^{-7}$ [71], still more than four orders of magnitude from the standard-model prediction.

The next generation of $K_L^0 \rightarrow \pi^0 \nu \bar{\nu}$ experiments will start with E391a (see Section 6.6) at the High Energy Accelerator Research Organization (KEK) in Tsukuba (Japan), which hopes to reach a sensitivity of $\sim 10^{-10}$. This experiment will use a technique similar to KTeV, with a pencil beam, high quality calorimetry and very efficient photon vetos. This experiment would eventually move to the Japanese Hadron Facility (JHF), a new 50 GeV proton accelerator that is expected to be built around 2006, and attempt to push to a sensitivity of $\mathcal{O}(10^{-14})$. Two other future experiments propose to reach sensitivities of

$\mathcal{O}(10^{-13})$: E926 (KOPIO/RSVP) at BNL (see Section 6.1.4) and E804 (KAMI) at FNAL (see Section 6.2.2). The KOPIO technique is significantly different from the others; all possible initial and final state quantities will be measured, including the K_L momentum and the photon times, energies and directions. A pre-radiator is used to reconstruct the directions of the two photons and a low momentum bunched beam is used to derive the kaon momentum from time of flight. This technique, which also relies on a very efficient photon veto system, has additional tools to reject backgrounds: the quality of the π^0 vertex and the π^0 momentum in the kaon center of mass.

The decays $K_L^0 \rightarrow \pi^+ \pi^- \nu \bar{\nu}$, $K_L^0 \rightarrow \pi^0 \pi^0 \nu \bar{\nu}$ and $K^+ \rightarrow \pi^+ \pi^0 \nu \bar{\nu}$ are also very clean theoretically and measurements of these branching ratios could be used to determine η and ρ [72]. Unfortunately, the SM expectations for these branching ratios are $\mathcal{O}(10^{-13})$, $\mathcal{O}(10^{-13})$ and $\mathcal{O}(10^{-14})$ respectively and are not accessible for precision measurements in current or next generation experiments. A limit on $K^+ \rightarrow \pi^+ \pi^0 \nu \bar{\nu}$ has recently been derived by E787: $B(K^+ \rightarrow \pi^+ \pi^0 \nu \bar{\nu}) < 4.3 \times 10^{-5}$ [73]. Table 3 summarizes the current experimental status of $K \rightarrow \pi \nu \bar{\nu}$.

Table 3: Summary of $K \rightarrow \pi \nu \bar{\nu}$ results

Decay Mode	Branching Ratio	events	Experiment
$K^+ \rightarrow \pi^+ \nu \bar{\nu}$	$(1.5_{-1.2}^{+3.4}) \times 10^{-10}$	1	E787 (2000) [68]
$K_L^0 \rightarrow \pi^0 \nu \bar{\nu}$	$< 1.6 \times 10^{-6}$	0	KTeV (2000) [70]
$K_L^0 \rightarrow \pi^0 \nu \bar{\nu} (ee\gamma)$	$< 5.9 \times 10^{-7}$	0	KTeV (2000) [71]
$K_L^0 \rightarrow \pi^0 \nu \bar{\nu} (\pi^+ \nu \bar{\nu})$	$< 2.6 \times 10^{-9}$	—	E787 (2000) [68]
$K^+ \rightarrow \pi^+ \pi^0 \nu \bar{\nu}$	$< 4.3 \times 10^{-5}$	0	E787 (2000) [73]

3 FORM FACTORS

In addition to the rare kaon decays that directly probe standard-model parameters (as discussed in the preceding section), and those that are sensitive to BSM physics (the subject of the following section), there is an impressively broad array of other decay modes on which substantial experimental progress has been made in recent years. Although these results receive less attention, they provide critical information in a variety of areas.

For example, there has historically been strong interest in the $K_L^0 \rightarrow \mu^+ \mu^-$ decay as a probe of weak interaction dynamics, specifically $Re(V_{td})$, through its short-distance amplitude. But the short-distance amplitude is known to be quite small compared with the long-distance part, involving the $\gamma\gamma$ and $\gamma^*\gamma^*$ intermediate states. An accurate determination of the $K_L\gamma^*\gamma^*$ form factor is needed in order to evaluate the long-distance contribution, which is needed in turn to extract $Re(V_{td})$ from $B(K_L^0 \rightarrow \mu^+ \mu^-)$. There are various theoretical models for the form factor, each involving parameters that must be determined from experiments discussed in Section 3.1.

The measurement of such modes as $K_L^0 \rightarrow \pi^0 \gamma\gamma$ and $K_L^0 \rightarrow e^+ e^- \gamma\gamma$ is important for a different reason. As discussed in Section 2.2, $K_L^0 \rightarrow \ell^+ \ell^- \gamma\gamma$ is an important background in the search for $K_L^0 \rightarrow \pi^0 \ell^+ \ell^-$. Both the absolute number of events from this process and the kinematic distributions of those events are

thus important to the effort to learn about standard-model parameters from $K_L^0 \rightarrow \pi^0 e^+ e^-$ and $K_L^0 \rightarrow \pi^0 \mu^+ \mu^-$. In particular, large samples of these events must be studied to determine the effectiveness of kinematic cuts necessary to observe this extremely rare decay. The decay $K_L^0 \rightarrow \pi^0 \gamma \gamma$, though not a background to $K_L^0 \rightarrow \pi^0 e^+ e^-$, can be used to determine the CP -conserving part of the amplitude. Additional contributions from the $\pi^0 \gamma^* \gamma^*$ intermediate state with off-shell photons are also important. These can be determined from ChPT models, but again there are undetermined parameters that must be extracted by studying kinematic distributions in $K_L^0 \rightarrow \pi^0 \gamma \gamma$ and the related mode $K_L^0 \rightarrow \pi^0 e^+ e^- \gamma$.

Because of their low energy release and wide variety of final states, kaon decays provide an excellent testing ground for the predictions of ChPT. For example, the $K \rightarrow \pi \gamma \gamma$ modes and the direct-emission component of radiative semileptonic decay modes have proven to be good testing grounds for comparing $\mathcal{O}(p^4)$ to $\mathcal{O}(p^6)$ calculations. ChPT calculations of $\pi\pi$ scattering can likewise be tested by measuring the form factors of $K \rightarrow \pi \pi \ell \nu_\ell$ ($K_{\ell 4}$) decays.

Sometimes the study of these less well-known modes can turn up new phenomena of considerable interest. For example, an interesting observation of a CP -violating and T -odd angular asymmetry in the $K_L^0 \rightarrow \pi^+ \pi^- e^+ e^-$ decay has been made by the NA48 and KTeV experiments. This is the largest CP -violating effect yet seen, and the first CP -violating effect ever observed in an angular distribution.

Recent reviews of the current state of radiative and semileptonic kaon decay measurements are available from the DAΦNE workshop [74,75].

3.1 $K_L^0 \rightarrow \gamma \gamma$ and Related Decays

Like the π^0 , the neutral kaons couple to two photons. The effective interaction term for the CP -conserving interaction between a pseudoscalar meson field P of mass M_P and the electromagnetic field $F_{\mu\nu}$ is given by

$$\mathcal{L} = \frac{if_{P\gamma\gamma}}{4M_P} \epsilon_{\mu\nu\lambda\sigma} F^{\mu\nu} F^{\lambda\sigma} P. \quad (21)$$

In terms of the polarizations ϵ_i and momenta k_i of the two photons, this vertex becomes

$$\mathcal{L} = -\frac{2if_{P\gamma\gamma}}{M_P} \epsilon_{\mu\nu\lambda\sigma} k_1^\mu \epsilon_1^\nu k_2^\lambda \epsilon_2^\sigma, \quad (22)$$

which leads to a $\gamma\gamma$ partial width of

$$\Gamma_{\gamma\gamma}(P) = \frac{f_{P\gamma\gamma}^2 M_P}{16\pi}. \quad (23)$$

The coupling $f_{K_S\gamma\gamma}$ is determined in $\mathcal{O}(p^4)$ ChPT, without any free parameters, leading to the prediction [76] $\text{B}(K_S^0 \rightarrow \gamma\gamma) = 2.0 \times 10^{-6}$. This is in good agreement with the experimental value [77] (see Table 4), although the experimental errors are still rather large.

The interaction term for two real photons can be extended to off-shell photons with nonzero k^2 . In this case, the coupling $f_{P\gamma^*\gamma^*}$ can depend on the two k^2 values. Typically, a form factor $F_{P\gamma\gamma}$ is introduced, so that

$$f_{P\gamma^*\gamma^*}(k_1^2, k_2^2) = f_{P\gamma\gamma} F_{P\gamma\gamma}(k_1^2, k_2^2), \quad (24)$$

Table 4: Summary of results on kaon decays to two photons and related modes

Decay Mode	Branching Ratio	events	Experiment
$K_S^0 \rightarrow \gamma\gamma$	$(2.4 \pm 0.9) \times 10^{-6}$	16	NA31-95 [77]
$K_L^0 \rightarrow \gamma\gamma$	$(5.92 \pm 0.15) \times 10^{-4}$	110000	NA31-87 [82]
$K_L^0 \rightarrow \mu^+\mu^-$	$(7.24 \pm 0.17) \times 10^{-9}$	6200	E871-00 [49]
$K_L^0 \rightarrow e^+e^-$	$(8.7_{-4.1}^{+5.7}) \times 10^{-12}$	4	E871-98 [50]
$K_L^0 \rightarrow e^+e^-\gamma$	$(1.06 \pm 0.02 \pm 0.02 \pm 0.04) \times 10^{-5}$	6854	NA48-99 [80]
$K_L^0 \rightarrow \mu^+\mu^-\gamma$	$(3.69 \pm 0.04 \pm 0.07) \times 10^{-7}$	9105	KTeV-00 [81]
$K_L^0 \rightarrow e^+e^-e^+e^-$	$(4.14 \pm 0.27 \pm 0.31) \times 10^{-8}$	300	KTeV-98 [83]
$K_L^0 \rightarrow \mu^+\mu^-e^+e^-$	$(2.50 \pm 0.41 \pm 0.16) \times 10^{-9}$	~40	KTeV-99 [84]
$K_L^0 \rightarrow \mu^+\mu^-\mu^+\mu^-$	no limit		
$K_S^0 \rightarrow \mu^+\mu^-$	$< 3.2 \times 10^{-7}$	0	CERN-73 [85]
$K_S^0 \rightarrow e^+e^-$	$< 1.4 \times 10^{-7}$	0	CPLEAR [86]
$K_L^0 \rightarrow e^+e^-\gamma\gamma$	$(6.31 \pm 0.14 \pm 0.42) \times 10^{-7}$	1911	KTeV-00 [87]
$K_L^0 \rightarrow \mu^+\mu^-\gamma\gamma$	$(1.42_{-0.81}^{+1.02} \pm 0.14) \times 10^{-9}$	4	KTeV-00 [88]

and the form factor is consequently normalized to the point $F_{P\gamma\gamma}(0,0) = 1$. The form factor $F_{K_L\gamma\gamma}$ is needed to accurately calculate the long-distance contribution to $K_L^0 \rightarrow \mu^+\mu^-$ and $K_L^0 \rightarrow e^+e^-$, which both have important contributions from the $\gamma^*\gamma^*$ intermediate state. As is discussed in Section 2.1, this long-distance contribution must be subtracted from the precise experimental measurement of $K_L^0 \rightarrow \mu^+\mu^-$ in order to determine the interesting short-distance part of the amplitude for that decay, which can be related to the real part of the CKM matrix element V_{td} or, equivalently, to the standard-model parameter ρ .

A number of models are available for the form factor. The simplest approach is to determine the coefficient of the first few terms in a Taylor series expansion in the parameters $x_i = k_i^2/M_K^2$. An alternative parameterization [43] assumes that the form factor can be written in terms of vector-meson poles with arbitrary residues:

$$F(k_1^2, k_2^2) = 1 + \alpha \left(\frac{k_1^2}{k_1^2 - M_V^2} + \frac{k_2^2}{k_2^2 - M_V^2} \right) + \beta \frac{k_1^2 k_2^2}{(k_1^2 - M_V^2)(k_2^2 - M_V^2)}. \quad (25)$$

Rare kaon decays can be used to study the $K\gamma\gamma$ form factors in several regions. For example, the electron and muon Dalitz decays $K_L^0 \rightarrow e^+e^-\gamma$ and $K_L^0 \rightarrow \mu^+\mu^-\gamma$ are sensitive to the form factor with $k_2^2 = 0$ and $4m^2 < k_1^2 < M_K^2$, where m^2 is the lepton mass. From lepton universality [78] the form factors obtained in the electron and muon modes should be the same. A new, high-precision result from KTeV (see Section 6.2.1) for $K_L^0 \rightarrow \mu^+\mu^-\gamma$ is available; the mass distribution of the final event sample collected during 1996–1997 is shown in Figure 10. As Table 4 shows, substantial statistics are now available in both of these $\ell\ell\gamma$ modes. Experiments analyzing $l^+l^-\gamma$ data have usually fit for the α_{K^*} parameter in the Bergström, Massó & Singer form factor model [79],

$$F(k^2, 0) = \frac{k^2}{k^2 - M_\rho^2} + \frac{2.5\alpha_{K^*} \cdot k^2}{k^2 - M_{K^*}^2} \left(\frac{4}{3} - \frac{k^2}{k^2 - M_\rho^2} - \frac{k^2/9}{k^2 - M_\omega^2} - \frac{2k^2/9}{k^2 - M_\phi^2} \right). \quad (26)$$

This model is based on a vector-dominance picture of pseudoscalar-pseudoscalar transitions (the first term) and vector-vector transitions involving K^*V vertices

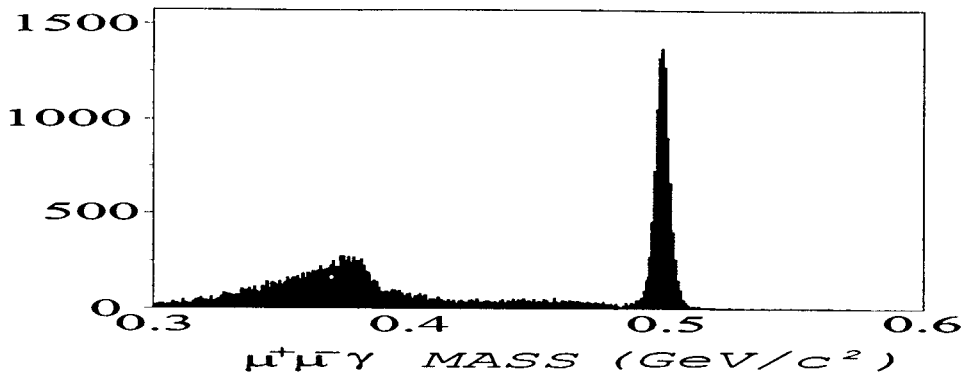


Figure 10: KTeV: Final $K_L^0 \rightarrow \mu^+ \mu^- \gamma$ data sample collected in 1996–1997 after all cuts. A total of 9105 $K_L^0 \rightarrow \mu^+ \mu^- \gamma$ events are observed in the peak.

(the second term). This form provides an acceptable fit to the data. Two recent fits based on high-statistics analyses yield rather different values, though. A recent fit [80] to the NA48 (see Section 6.3) $K_L^0 \rightarrow e^+ e^- \gamma$ data yields $\alpha_{K^*} = -0.36 \pm 0.06$, somewhat more negative than the best fit values from earlier experiments studying the same mode. A new KTeV result [81] based on the $K_L^0 \rightarrow \mu^+ \mu^- \gamma$ mode finds $\alpha_{K^*} = -0.17 \pm 0.03$, a value about three sigma different from the new NA48 result. The k^2 region sampled by the $K_L^0 \rightarrow \mu^+ \mu^- \gamma$ data is much more heavily weighted to large k^2 values, such that a different form factor model might reduce the discrepancy.

The rarer double-internal-conversion modes, where the final state consists of two lepton pairs, are sensitive to the form factor in the region $4m_1^2 < k_1^2 < (M_K - 2m_2)^2$ and $4m_2^2 < k_2^2 < (M_K - 2m_1)^2$, where m_1 and m_2 are the two lepton masses. Three such modes are expected: $K_L^0 \rightarrow e^+ e^- e^+ e^-$, $K_L^0 \rightarrow \mu^+ \mu^- e^+ e^-$ and $K_L^0 \rightarrow \mu^+ \mu^- \mu^+ \mu^-$. The production of muon pairs requires virtual photons at much higher k^2 and is strongly suppressed. The largest sample of $e^+ e^- e^+ e^-$ decays reported to date is from KTeV, with 440 events in the 1997 data sample. KTeV has also reported seeing about 40 $e^+ e^- \mu^+ \mu^-$ events. The predicted branching ratio for the $K_L^0 \rightarrow \mu^+ \mu^- \mu^+ \mu^-$ mode is below 10^{-12} , two orders of magnitude beyond the sensitivity of KTeV.

Two decay modes related to $K_L^0 \rightarrow \gamma\gamma$, though not especially interesting in themselves, have significant implications for the attempt to observe direct CP violation in $K_L^0 \rightarrow \pi^0 e^+ e^-$ and $K_L^0 \rightarrow \pi^0 \mu^+ \mu^-$. These are the radiative Dalitz decays $K_L^0 \rightarrow e^+ e^- \gamma\gamma$ and $K_L^0 \rightarrow \mu^+ \mu^- \gamma\gamma$. With a typical infrared cutoff of 5 MeV for the photon energies in the kaon center of mass, the electron mode, $K_L^0 \rightarrow e^+ e^- \gamma\gamma$, has a branching ratio of about 6×10^{-7} , five orders of magnitude higher than the expected rate for $K_L^0 \rightarrow \pi^0 e^+ e^-$. Moreover, the peak of the $\gamma\gamma$ invariant mass spectrum in observed events is near the π^0 mass. With a good calorimeter, experiments can limit the π^0 mass range to a few MeV, but the number of $e^+ e^- \gamma\gamma$ events in this range still swamps the expected $\pi^0 e^+ e^-$ signal. Further reduction in this background can be achieved by cutting on kinematic variables to remove, for example, events in which the momentum of one of the photons is nearly parallel to that of one of the leptons; this topology is typical of radiative Dalitz decays but uncommon for $\pi^0 e^+ e^-$ events. But even an optimal set of cuts cannot reduce

this background to the level of the expected signal, a major impediment to the measurement of $B(K_L^0 \rightarrow \pi^0 e^+ e^-)$. KTeV has identified a sample of over 1500 $e^+ e^- \gamma \gamma$ events and has verified that their kinematic distributions are generally in agreement with those predicted.

The decay $K_L^0 \rightarrow \mu^+ \mu^- \gamma \gamma$ is likewise a serious background to the measurement of $K_L^0 \rightarrow \pi^0 \mu^+ \mu^-$. The absolute rate for this decay is much less than the rate for the corresponding electron mode (see Table 4). Unfortunately, the part of the phase space where this decay can be a background to $K_L^0 \rightarrow \pi^0 \mu^+ \mu^-$, after the $M_{\gamma\gamma}$ and other kinematic cuts, is not particularly suppressed. Thus, the $K_L^0 \rightarrow \pi^0 \mu^+ \mu^-$ mode does not allow experiments to eliminate the radiative Dalitz background.

Table 4 summarizes results of kaon decays to two real or off-shell photons. With completion of the KTeV analysis, the $K_L^0 \rightarrow \ell^+ \ell^- \gamma$ modes should be improved by more than a factor of two. The $K_L^0 \rightarrow \ell^+ \ell^- e^+ e^-$ data should triple. The K_S modes may be improved by NA48 in a dedicated experiment after the ϵ'/ϵ running. The $K_L^0 \rightarrow \gamma \gamma$ and $K_S^0 \rightarrow \gamma \gamma$ as well as several other modes will be improved by KLOE. No improvements are expected for $K_L^0 \rightarrow \mu^+ \mu^-$ or $K_L^0 \rightarrow e^+ e^-$ in the foreseeable future.

3.2 $K \rightarrow \pi \gamma \gamma$

The decay rate and spectral shape of $K_L^0 \rightarrow \pi^0 \gamma \gamma$ are calculated at $\mathcal{O}(p^4)$ of ChPT, without any free parameters [76]. The prediction of the spectral shape is a striking success of ChPT. However, the decay rate is a factor of three too small. To match the experimental value, a model-dependent contribution from $\mathcal{O}(p^6)$ is needed, which is usually parameterized with a constant a_V [89], that measures the vector meson exchange contribution to the amplitude. This parameter is of particular importance because the CP -conserving contribution to $K_L^0 \rightarrow \pi^0 e^+ e^-$ depends on the value of a_V . Based on half of the total data sample, KTeV (see Section 6.2.1) has recently measured $a_V = -0.72 \pm 0.05 \pm 0.06$ [90], implying a contribution of $1-2 \times 10^{-12}$ to $K_L^0 \rightarrow \pi^0 e^+ e^-$. NA48 has also reported a preliminary result [91], based on almost 1400 events from part of the 1998 and 1999 runs, of $B(K_L^0 \rightarrow \pi^0 \gamma \gamma) = (1.51 \pm 0.05 \pm 0.20) \times 10^{-6}$, with $a_V = -0.45$.

Calculation for the charged mode $K^+ \rightarrow \pi^+ \gamma \gamma$ is more complicated, requiring an unknown parameter, \hat{c} [92,93], even at $\mathcal{O}(p^4)$; however, it also provides a good test of ChPT [94]. Both the decay rate and spectral shape are predicted with this single parameter. As with $K_L^0 \rightarrow \pi^0 \gamma \gamma$, the two-photon invariant mass ($M_{\gamma\gamma}$) peaks above the two-pion mass, $M_{\pi^+ \pi^-}$, implying an intermediate $K^+ \rightarrow \pi^+ \pi^+ \pi^-$ decay. This observation has led to improved ChPT predictions, normalizing to the $K^+ \rightarrow \pi^+ \pi^+ \pi^-$ measurement—the so-called unitarity corrections [95]. E787 (see Section 6.1.3) has measured a branching ratio [96] of $B(K^+ \rightarrow \pi^+ \gamma \gamma) = (6.0 \pm 1.5 \pm 0.7) \times 10^{-7} (100 < P_{\pi^+} < 180 \text{ MeV}/c)$ and $\hat{c} = 1.8 \pm 0.6$. The data favor unitarity corrections.

Table 5 summarizes the experimental measurements of $K \rightarrow \pi \gamma \gamma$. The KTeV measurement of $K_L^0 \rightarrow \pi^0 e^+ e^- \gamma$ should improve by a factor of three; the measurement of $K_L^0 \rightarrow \pi^0 \gamma \gamma$ should improve by a factor of two. Additional improvements will await the next round of experiments, including a possible search for $K_S^0 \rightarrow \pi^0 \gamma \gamma$ by NA48 after the ϵ'/ϵ running is completed.

Table 5: Summary of $K \rightarrow \pi\gamma\gamma$ results

Decay Mode	Branching Ratio	events	Experiment
$K_L^0 \rightarrow \pi^0\gamma\gamma$	$(1.68 \pm 0.07 \pm 0.08) \times 10^{-6}$	884	KTeV (1999) [90]
$K^+ \rightarrow \pi^+\gamma\gamma$	$(6.0 \pm 1.5 \pm 0.7) \times 10^{-7}$	26	E787 (1997) [96]
$K_L^0 \rightarrow \pi^0 e^+ e^- \gamma$	$(2.20 \pm 0.48 \pm 0.11) \times 10^{-8}$	18	KTeV (1999) [97]

3.3 $K^+ \rightarrow \pi^+ \ell^+ \ell^-$

The $K^+ \rightarrow \pi^+ \ell^+ \ell^-$ decays are suppressed in the standard model, since they proceed via a flavor-changing neutral current: an effective Zds coupling that is forbidden in the SM at tree-level, but permitted at the one-loop level. However, they are dominated by long-distance effects and proceed electromagnetically through single-photon exchange, so it is not possible to extract short-distance physics from these modes (unless one measures the lepton polarization). These decays have been extensively studied within ChPT [51,92,93,98]. To $\mathcal{O}(p^4)$ in ChPT, the rate and di-lepton invariant mass spectra ($M_{\ell^+\ell^-}$) for both $K^+ \rightarrow \pi^+ e^+ e^-$ and $K^+ \rightarrow \pi^+ \mu^+ \mu^-$ are described by one free parameter, w_+ . This parameter has been calculated in various models [92]. At $\mathcal{O}(p^6)$ in ChPT, additional parameters are needed; w_+ is replaced by a_+ and b_+ [99].

The $K^+ \rightarrow \pi^+ e^+ e^-$ decay was first observed in the 1970s [100], and since that time a series of experiments at BNL has increased the event sample substantially [101-103]. The most recent experiment, E865 [103] (see Section 6.1.1), reported a branching ratio of $B(K^+ \rightarrow \pi^+ e^+ e^-) = (2.94 \pm 0.05 \pm 0.13 \pm 0.05) \times 10^{-7}$, based on 10,175 events. (The errors are statistical, systematic, and from the theoretical uncertainty of the spectral shape.) A fit to the $M_{e^+e^-}$ spectra gives values for the form factor parameters of

$$a_+ = -0.587 \pm 0.010, \quad b_+ = -0.655 \pm 0.044. \quad (27)$$

The first observation of the decay $K^+ \rightarrow \pi^+ \mu^+ \mu^-$ was reported by E787 (see Section 6.1.3) in 1997 [104]. A total of 200 events were recorded during the 1989–1991 running period. The branching ratio was measured to be $B(K^+ \rightarrow \pi^+ \mu^+ \mu^-) = (5.0 \pm 0.4 \pm 0.7 \pm 0.6) \times 10^{-8}$. This mode has subsequently been observed by E865 [105], with 430 events and a measured branching ratio of $B(K^+ \rightarrow \pi^+ \mu^+ \mu^-) = (9.22 \pm 0.60 \pm 0.49) \times 10^{-8}$. Because all events are fully reconstructed, a measurement of the $\mu\mu$ invariant mass ($M_{\mu\mu}$) is possible. This most recent measurement disagrees with the previous one by more than 3σ , for reasons that are not yet understood.

Table 6 summarizes the experimental measurements of $K^+ \rightarrow \pi^+ \ell^+ \ell^-$.

Table 6: Summary of $K^+ \rightarrow \pi^+ \ell^+ \ell^-$ results

Decay Mode	Branching Ratio	events	Experiment
$K^+ \rightarrow \pi^+ e^+ e^-$	$(2.94 \pm 0.05 \pm 0.13) \times 10^{-7}$	10300	E865 (1999) [103]
$K^+ \rightarrow \pi^+ \mu^+ \mu^-$	$(9.22 \pm 0.60 \pm 0.49) \times 10^{-8}$	430	E865 (2000) [105]
$K^+ \rightarrow \pi^+ e^+ e^- \gamma$	—	~30	E865 (1999) [106]

3.4 $K \rightarrow \pi\pi\gamma$

The radiative $K_{\pi 2}$ decays— $K^+ \rightarrow \pi^+\pi^0\gamma$, $K_L^0 \rightarrow \pi^+\pi^-\gamma$, and $K_S^0 \rightarrow \pi^+\pi^-\gamma$ —have two contributions. In the inner bremsstrahlung (IB) process, a photon is radiated from one of the charged particles. In the direct emission (DE) process, the photon is radiated from an intermediate state. The branching ratio of the IB contribution scales with the underlying $K_{\pi 2}$ decay rate. The DE decay probes the kaon structure and has been studied extensively in ChPT [107]. In K_L , IB is highly suppressed because the underlying decay is CP violating; in K^+ , it is somewhat suppressed due to the $\Delta I = 1/2$ rule; in K_S , it is not suppressed.

The decay $K_L^0 \rightarrow \pi^+\pi^-\gamma$ (DE) [108-110] has a long history. A new result [111] from KTeV (see Section 6.2.1) has recently been reported. The branching ratio for the DE component is $B(K_L^0 \rightarrow \pi^+\pi^-\gamma; \text{DE}, E_\gamma^* > 20 \text{ MeV}) = (3.70 \pm 0.10) \times 10^{-5}$. The fraction of DE is $\text{DE}/(\text{DE}+\text{IB}) = 0.685 \pm 0.009 \pm 0.017$. This result is based on $\sim 5\%$ of the total KTeV data for this mode.

The charged mode, $K^+ \rightarrow \pi^+\pi^0\gamma$, also has a long history [112-114]. New results from E787 [115] (see Section 6.1.3) are striking in that the DE branching ratio is a factor of four lower than the previous value. The data are traditionally expressed in terms of the variable W that behaves similarly to the photon energy, and which is defined as

$$\begin{aligned} W^2 &\equiv (p \cdot q)/m_{K^+}^2 \times (p_+ \cdot q)/m_{\pi^+}^2 \\ &= E_\gamma^2 \times (E_{\pi^+} - P_{\pi^+} \times \cos \theta_{\pi^+ \gamma}) / (m_{K^+} \times m_{\pi^+}), \end{aligned} \quad (28)$$

where p is the four momentum of the kaon, q is the four momentum of the photon and p_+ is the four momentum of the π^+ . The new result from E787, based on half of the total data set, shown in Figure 11, has about eight times higher statistics than previous results. The branching ratio for the DE component, from a fit to IB

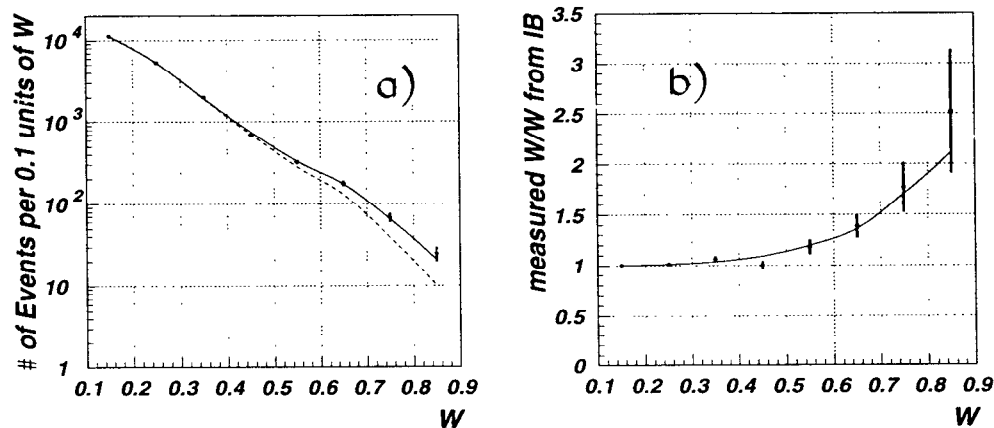


Figure 11: E787: a) The measured W spectrum for signal events compared to best fits to IB+DE (solid curve) and IB alone (dashed curve); b) The ratio of the measured W spectrum to the predicted IB spectrum.

and DE, is $B(K^+ \rightarrow \pi^+\pi^0\gamma; \text{DE}, 55 < T_{\pi^+} < 90 \text{ MeV}) = (4.72 \pm 0.77 \pm 0.28) \times 10^{-6}$. The interference term is small, $(-0.4 \pm 1.6)\%$, and the DE is $(1.85 \pm 0.30)\%$ compared with the IB term. The decay rate, corrected to full phase space,¹ is

¹This correction assumes that the form factor has no energy dependence.

now measured to be similar to that for K_L : $\Gamma(K^+ \rightarrow \pi^+\pi^0\gamma; DE) = 808 \pm 132 s^{-1}$ vs. $\Gamma(K_L^0 \rightarrow \pi^+\pi^-\gamma; DE) = 617 \pm 18 s^{-1}$.

In the neutral kaon decay, $K_L^0 \rightarrow \pi^+\pi^-\gamma$, the DE part of the decay can be either CP -violating or CP -conserving, but experiments show that the DE decay is consistent with a CP -conserving M1 radiative transition. There is also a CP -odd interference term. These CP -odd and CP -even terms manifest themselves in a CP -violating asymmetry in the polarization of the photon, which is not observable in these experiments. However, a CP - and T -odd angular asymmetry is expected in the related decay $K_L^0 \rightarrow \pi^+\pi^-e^+e^-$, in which the photon internally converts to an e^+e^- pair, since the angular distribution of the leptons preserves information about the photon polarization. This effect, predicted in 1992 by Sehgal & Wanninger [116], is an asymmetry in the distribution of the angle ϕ between the two planes formed by the lepton momenta and the pion momenta in the K_L rest frame. The predicted asymmetry [116,117] is quite large because the two interfering amplitudes are of comparable size.

NA48 reports [118] (see Section 6.3) a signal of 458 events, over 37 background events, giving a preliminary branching ratio of $B(K_L^0 \rightarrow \pi^+\pi^-e^+e^-) = (2.90 \pm 0.15) \times 10^{-7}$. In 1998, KTeV published a branching ratio [119] based on a small subset of the 1997 data. A new result from the full 1997 data set, with over 1500 events, has now been reported [120], $B(K_L^0 \rightarrow \pi^+\pi^-e^+e^-) = (3.63 \pm 0.11 \pm 0.14) \times 10^{-7}$. The branching ratio is larger than the one reported by NA48, but the difference is mostly due to the inclusion of an M1 form factor, which is not used in the NA48 analysis and which significantly increases the measured value by reducing the acceptance. Figure 12a shows the invariant mass spectrum observed by KTeV.

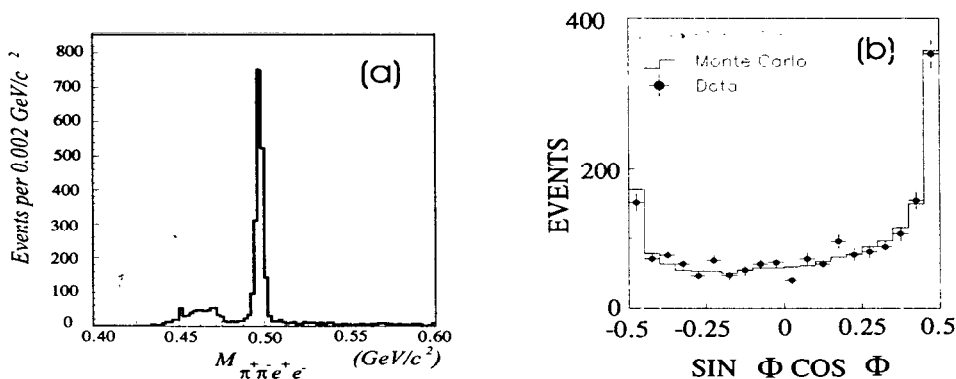


Figure 12: KTeV: a) Distribution of invariant mass for $\pi^+\pi^-e^+e^-$ events. b) Distribution of the angle ϕ between the e^+e^- and $\pi^+\pi^-$ planes in the K_L rest frame. The asymmetry observed between negative and positive values of $\sin\phi\cos\phi$ is CP -violating and T -odd.

Both experiments observe a very large CP -violating and T -odd asymmetry. The asymmetry is defined by

$$A_\phi = \frac{N(\sin\phi\cos\phi > 0) - N(\sin\phi\cos\phi < 0)}{N(\sin\phi\cos\phi > 0) + N(\sin\phi\cos\phi < 0)}. \quad (29)$$

It is important to note that the raw asymmetry may be significantly different from the acceptance-corrected asymmetry. This occurs not because of any asymmetry in the detectors but because the asymmetry varies across the phase space for the $\pi^+\pi^-e^+e^-$ final state, and in general, acceptance is better in regions of the phase space where the asymmetry is large.

The raw asymmetries observed by the two experiments are therefore not directly comparable. Nevertheless, they seem to agree. NA48 finds $A_\phi(\text{raw}) = (20 \pm 5)\%$ while KTeV measures $A_\phi(\text{raw}) = (23.3 \pm 2.3)\%$. The angular distribution observed by KTeV is shown in Figure 12b.

So far, only KTeV has reported an acceptance-corrected asymmetry [121]. An important ingredient in making the acceptance correction is the form factor in the M1 DE amplitude, which is extracted by fitting the $M_{\pi\pi}$ and other kinematic distributions. Using the fitted form factor, the acceptance-corrected average asymmetry is found to be

$$A_\phi(\text{corrected}) = (13.6 \pm 2.5 \pm 1.2)\%, \quad (30)$$

in excellent agreement with the theoretical prediction based on the value of the indirect CP -violation parameter η_{+-} and the known $\pi\pi$ phase shifts.

The NA48 experiment has reported the first observation of $K_S^0 \rightarrow \pi^+\pi^-e^+e^-$ from the 1998 data sample [122] (see Table 7). An additional 730 events were observed

Table 7: Summary of radiative $K_{\pi 2}$ results

Decay Mode	Branching Ratio	events	Experiment
$K_L^0 \rightarrow \pi^+\pi^-\gamma$ (DE)	$(3.70 \pm 0.10) \times 10^{-5}$	5900	KTeV (2000) [111]
$K^+ \rightarrow \pi^+\pi^0\gamma$ (DE)	$(4.72 \pm 0.77 \pm 0.28) \times 10^{-6}$	360	E787 (2000) [115]
$K_L^0 \rightarrow \pi^+\pi^-e^+e^-$	$(3.63 \pm 0.11 \pm 0.14) \times 10^{-7}$	1500	KTeV (1998) [119]
$K_S^0 \rightarrow \pi^+\pi^-e^+e^-$	4×10^{-5}	58	NA48 (2000) [122]
$K_L^0 \rightarrow \pi^0\pi^0\gamma$	$< 5.6 \times 10^{-6}$	0	NA31 (1994) [123]
$K_S^0 \rightarrow \pi^+\pi^-\gamma$	$(1.78 \pm 0.05) \times 10^{-3}$	3700	E731 (1993) [110]
$K_S^0 \rightarrow \pi^+\pi^-\gamma$ (DE)	$< 0.06 \times 10^{-3}$	0	CERN (1976) [109]

in a special two day K_S run in 1999. The raw asymmetry is consistent with 0, as expected for K_S . Table 7 summarizes the current experimental status of radiative $K_{\pi 2}$ decays.

3.5 Radiative $K_{\ell 2}$ Decays

As with $K \rightarrow \pi\pi\gamma$, the radiative decays $K^+ \rightarrow \ell^+\nu\gamma$ and $K^+ \rightarrow \ell^+\nu\ell'^+\ell'^-$ proceed via two separate mechanisms. The first, IB, is the radiative version of the familiar $K^+ \rightarrow \ell^+\nu$ decays. The second, structure dependent (SD), as with the DE process in $K \rightarrow \pi\pi\gamma$, involves the emission of a photon from an intermediate state and has been studied extensively within the framework of ChPT [124,125]. The IB amplitude is completely determined by the kaon decay constant f_K . The SD amplitude is parametrized in terms of the three form factors F_V , F_A and R . The vector (\mathcal{A}_V) and axial-vector (\mathcal{A}_A) contributions are given by

$$\mathcal{A}_V = \frac{-eG_F V_{us}}{\sqrt{2}M_K} \epsilon^\mu \ell^\nu F_V e_{\mu\nu\sigma\tau} q^\sigma k^\tau \quad (31)$$

$$A_A = \frac{-ieG_F V_{us}}{\sqrt{2}M_K} F_A [(kq - q^2)g_{\mu\nu} - k_\mu q_\nu] + Rq^2 g_{\mu\nu}, \quad (32)$$

where ϵ^μ is the photon polarization, ℓ^ν is the lepton current and k and q are the kaon and photon 4-momentum. In $\mathcal{O}(p^4)$ of ChPT, the form factors are independent of q^2 , although in $\mathcal{O}(p^6)$ they take on a q^2 dependence.

Recent measurements should allow precise experimental determinations of all three parameters. The most recent determination of $|F_V + F_A| = 0.165 \pm 0.007 \pm 0.011$ from the E787 (see Section 6.1.3) measurement [126] of the DE component of $K^+ \rightarrow \mu^+ \nu_\mu \gamma$ is consistent with the previous determination [127] of $|F_V + F_A| = 0.148 \pm 0.010$ from $K^+ \rightarrow e^+ \nu_e \gamma$. The branching ratio for the structure-dependent component of $K^+ \rightarrow \mu^+ \nu_\mu \gamma$, $B(K^+ \rightarrow \mu^+ \nu_\mu \gamma; SD^+) = (1.33 \pm 0.12 \pm 0.18) \times 10^{-5}$, is about 40% higher than the $\mathcal{O}(p^4)$ ChPT calculation [125], but the $\mathcal{O}(p^6)$ contributions are expected to increase the calculation by a comparable amount (based on the $\mathcal{O}(p^6)$ calculation for $\pi^+ \rightarrow \ell^+ \nu_\ell \gamma$) [128]. A value of $F_V - F_A = 0.102 \pm 0.073 \pm 0.044$, also derived from the recent E787 $K^+ \rightarrow \mu^+ \nu_\mu \gamma$ (SD^+) measurement, is an improvement on the previous limit of $-0.3 < F_V - F_A < 2.5$ [129] (see Reference [126] for a discussion of the sign convention).

An improved measure of $F_V - F_A$, along with measurements $F_V + F_A$ and the first measurement of R in K^+ decays, is now available from the E865 (see Section 6.1.1) measurements of $K^+ \rightarrow e^+ \nu_e e^-$ and $K^+ \rightarrow \mu^+ \nu_\mu e^-$ [130]. These data were collected along with the $K^+ \rightarrow \pi^+ e^+ e^-$ data set in 1995–1996. The preliminary results from the combination of both modes are (statistical errors only) $F_V - F_A = 0.073 \pm 0.033$, $F_V + F_A = 0.143 \pm 0.027$ and $R = 0.233 \pm 0.016$. Combining the results on radiative $K^+ \rightarrow \ell^+ \nu$ decays, all three form factors, F_V , F_A and R , will be well determined, along with their sign relative to IB.

The E865 experiment has also observed some few dozen $K^+ \rightarrow e^+ \nu \mu^+ \mu^-$ events, collected along with the $K^+ \rightarrow \pi^+ \pi^- e^+ \nu_e$ data in 1997 [131] (see Section 3.6). A summary of the recent radiative $K_{\ell 2}$ results is presented in Table 8.

Table 8: Summary of radiative $K_{\ell 2}$ results

Decay Mode	Branching Ratio	events	Experiment
$K^+ \rightarrow \mu^+ \nu_\mu \gamma$	$(5.50 \pm 0.28) \times 10^{-3}$		KEK (1985) [129]
$K^+ \rightarrow \mu^+ \nu_\mu \gamma$ (DE)	$(1.33 \pm 0.12 \pm 0.18) \times 10^{-5}$	2588	E787 (2000) [126]
$K^+ \rightarrow e^+ \nu_e \gamma$ (DE)	$(1.52 \pm 0.23) \times 10^{-5}$	51	CERN (1979) [127]
$K^+ \rightarrow \mu^+ \nu \mu^+ \mu^-$	$< 4.1 \times 10^{-7}$	0	E787 (1989) [132]
$K^+ \rightarrow e^+ \nu \mu^+ \mu^-$	$< 5.0 \times 10^{-7}$	0	E787 (1998) [133]
$K^+ \rightarrow \mu^+ \nu e^+ e^-$	$(6.84 \pm 0.40) \times 10^{-8}$	~ 1500	E865 (2000) [130]
$K^+ \rightarrow e^+ \nu e^+ e^-$	$(2.60 \pm 0.15) \times 10^{-8}$	~ 400	E865 (2000) [130]

3.6 $K \rightarrow \pi \pi e \nu_e$

The $K^+ \rightarrow \pi^+ \pi^- e^+ \nu_e$ decay provides the best system for study of $\pi\pi$ scattering at low energy. The measurement of the relative phase of the pion wave functions is an important test for ChPT, as $\pi\pi$ scattering is uniquely sensitive to chiral symmetry breaking in the strong interaction and can provide powerful constraints on the parameters of ChPT. The ChPT calculations of $\pi\pi$ scattering have been done to $\mathcal{O}(p^4)$ [37,134] and $\mathcal{O}(p^6)$ [135].

The primary motivation for studying $K^+ \rightarrow \pi^+ \pi^- e^+ \nu_e$ is to measure this $\pi\pi$ scattering. The previous experiment had $\sim 30,000$ events [136]. The E865 experiment (see Section 6.1.1) has collected $\sim 400,000$ events. Figure 13 shows a preliminary plot of the $\pi\pi$ phase shift ($\delta \equiv \delta_0^0 - \delta_1^1$) as a function of $\pi\pi$ invariant mass ($M_{\pi\pi}$) for the new E865 data [137] and the previous Rosselet data. The preliminary E865 result, from a fit to an improved functional form [138], gives a scattering length of $a_0^0 = 0.235 \pm 0.013(stat)$ [139]. In principle, $\pi\pi$ phase

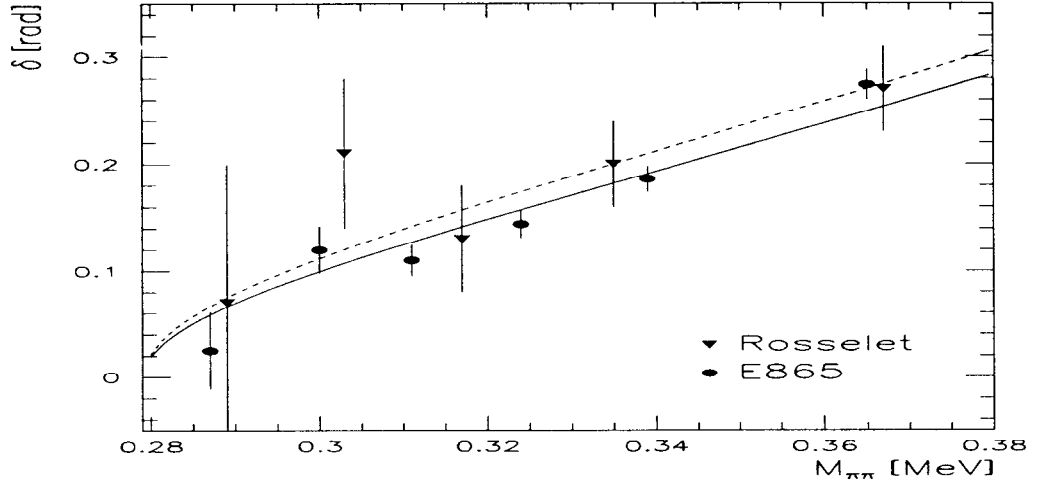


Figure 13: Preliminary $\pi\pi$ phase shift (δ) vs $\pi\pi$ invariant mass ($M_{\pi\pi}$). Both older data from Rosselet [136] and recent data from E865 [137] are shown, along with fits based on the Roy equation formalism of Basdevant, Froggatt & Petersen [140].

shifts could be extracted from the decay $K_L^0 \rightarrow \pi^\pm \pi^\circ e^\mp \nu_e$, or from the modes, $K^+ \rightarrow \pi^+ \pi^- \mu^+ \nu_\mu$, $K_L^0 \rightarrow \pi^\circ \pi^\pm \mu^\mp \nu_\mu$. However, due to limited statistics in these modes, they have not contributed significantly. Table 9 gives a summary of $K_{\mu 4}$ decays. E865 has collected $K^+ \rightarrow \pi^+ \pi^- e^+ \nu_e \gamma$ events as part of the study of

Table 9: Summary of $K_{\mu 4}$ results

Decay Mode	Branching Ratio	events	Experiment
$K^+ \rightarrow \pi^+ \pi^- e^+ \nu_e$	$(4.10 \pm 0.01 \pm 0.11) \times 10^{-5}$	> 350000	E865 (2000) [139]
$K^+ \rightarrow \pi^+ \pi^- \mu^+ \nu_\mu$	$(1.4 \pm 0.9) \times 10^{-5}$	7	CERN (1967) [141]
$K_L^0 \rightarrow \pi^\pm \pi^\circ e^\mp \nu_e$	$(5.16 \pm 0.20 \pm 0.22) \times 10^{-5}$	729	E799 (1993) [142]
$K^+ \rightarrow \pi^\circ \pi^\circ e^+ \nu_e$	$(2.1 \pm 0.4) \times 10^{-5}$	10	ITEP (1988) [143]
$K^+ \rightarrow \pi^\circ \pi^\circ e^+ \nu_e \gamma$	$< 5 \times 10^{-6}$	0	ITEP (1992) [144]

$K^+ \rightarrow \pi^+ \pi^- e^+ \nu_e$ and may report on this observation in the near future.

3.7 Other Rare or Radiative Decays

3.7.1 Rare K_S Decays

The CPLEAR experiment studies $p\bar{p}$ annihilation at low energy leading to the final state $K^+ \pi^- \bar{K}^0$ and its charge conjugate $K^- \pi^+ K^0$. The sign of the charged

kaon allows the neutral kaon to be tagged as either a K^0 or a \bar{K}^0 . Detailed measurements of the proper time decay distributions for these states to a particular final state allow extraction of a variety of parameters describing both K_L and K_S decays to each final state.

This technique allows the indirect determination of some rare K_S decays. Most notably, CPLEAR has recently studied the $\pi^+\pi^-\pi^0$ final state, a common K_L decay [145]. By fitting the proper time decay distributions for initial K^0 and \bar{K}^0 , and fitting the Dalitz plot distributions of these events, one can determine both CP -conserving and CP -violating amplitudes for $K_S^0 \rightarrow \pi^+\pi^-\pi^0$. The CP -violating amplitude is found to be consistent with zero, but the CP -conserving amplitude is observed with a three- to four-sigma significance. CPLEAR has converted this observation to a branching ratio [145] $B(K_S^0 \rightarrow \pi^+\pi^-\pi^0) = (2.5_{-1.0}^{+1.3+0.5}) \times 10^{-7}$. Although it is an indirect measurement, this is the smallest K_S branching ratio yet reported.

A new limit on $K_S^0 \rightarrow \pi^0\pi^0\pi^0$ has recently been presented by the SND experiment at VEPP-2M in Novosibirsk: $B(K_S^0 \rightarrow \pi^0\pi^0\pi^0) < 1.4 \times 10^{-5}$ [146].

3.7.2 Radiative Three-Body Decays

The experimental results for other radiative kaon decays (e.g. $K_{\pi 3\gamma}$ and $K_{\ell 3\gamma}$) are only sensitive to IB contributions. All of these measurements are consistent with theoretical predictions. A summary of these measurements is given in Table 10. The $K^+ \rightarrow \pi^0\mu^+\nu_\mu\gamma$ mode should be seen for the first time in existing data from

Table 10: Summary of radiative and rare three-body decays

Decay Mode	Branching Ratio	events	Experiment
$K_S^0 \rightarrow \pi^+\pi^-\pi^0$	$(2.5_{-1.0}^{+1.3+0.5}) \times 10^{-7}$		CPLEAR (1997) [145]
$K_S^0 \rightarrow \pi^0\pi^0\pi^0$	$< 1.4 \times 10^{-5}$	0	SND (1999) [146]
$K^+ \rightarrow \pi^+\pi^+\pi^-\gamma$	$(1.04 \pm 0.31) \times 10^{-4}$	7	ITEP (1989) [147]
$K^- \rightarrow \pi^-\pi^0\pi^0\gamma$	$(7.5_{-3.0}^{+5.5}) \times 10^{-6}$	5	IHEP (1995) [148]
$K^+ \rightarrow \pi^0\mu^+\nu_\mu\gamma$	$< 6.1 \times 10^{-5}$	0	ZGS (1973) [149]
$K_L^0 \rightarrow \pi^\pm\mu^\mp\nu_\mu\gamma$	$(5.7_{-0.7}^{+0.6}) \times 10^{-4}$	252	NA48 (1998) [150]
$K^+ \rightarrow \pi^0e^+\nu_e\gamma$	$(2.62 \pm 0.20) \times 10^{-4}$	88	ITEP (1991) [151]
$K^+ \rightarrow \pi^0e^+\nu_e\gamma$ (SD)	$< 5.3 \times 10^{-5}$	0	IHEP (1986) [152]
$K_L^0 \rightarrow \pi^\pm e^\mp\nu_e\gamma$	$(3.62_{-0.21}^{+0.26}) \times 10^{-4}$	1384	NA31 (1996) [153]

E787. Improvements in other modes are likely to come from KLOE and the Institute for High Energy Physics (IHEP) at Serpukhov.

4 LEPTON FLAVOR VIOLATION

All experimental evidence to date supports the exact conservation of an additive quantum number for each family of charged leptons. Thus $K_L^0 \rightarrow \mu^+\mu^-$ and $K_L^0 \rightarrow e^+e^-$ are allowed, although suppressed by the GIM mechanism and by helicity suppression, whereas $K_L^0 \rightarrow \mu e$ appears to be absolutely forbidden. If neutrino masses are nonzero, some very tiny mixing effects could permit such a decay in the standard model, but it would occur at unobservably small levels, many orders of magnitude beyond the present experimental sensitivity. Any observation

of a signal for the decays $K_L^0 \rightarrow \mu e$, $K^+ \rightarrow \pi^+ \mu^+ e^-$, or $K_L^0 \rightarrow \pi^0 \mu e$ would thus be conclusive evidence for new physics beyond the standard model [154].

Although this lepton-flavor-number conservation law appears to be respected in the standard model, there is no fundamental reason or underlying symmetry to explain why this should be so. Indeed, many possible extensions to the standard model predict new interactions involving heavy intermediate gauge bosons that could mediate the otherwise forbidden LFV decays. Some of the specific models that lead to LFV decays include [155] compositeness of quarks and leptons, left-right symmetric models, technicolor, some supersymmetric models, unified theories with horizontal gauge bosons, leptoquarks, and string theories.

It is important to look for both $K_L^0 \rightarrow \mu e$ and the modes with an extra pion, $K^+ \rightarrow \pi^+ \mu^+ e^-$ and $K_L^0 \rightarrow \pi^0 \mu e$, because the $K_L^0 \rightarrow \mu e$ decay is sensitive to pseudoscalar and axial vector coupling, whereas the other modes are sensitive to scalar or vector couplings. In both cases, the excellent sensitivity of these experiments probes mass scales that are very large. Of course, the sensitivity of the experiments to new interactions depends on the coupling constants involved. If the new coupling for an intermediate vector boson of mass M_X is g_X , then the lower bound on M_X implied by an upper limit on $B(K_L^0 \rightarrow \mu e)$ is given in terms of the electroweak coupling g by the approximate expression

$$M_X \simeq 200 \text{TeV}/c^2 \times \frac{g_X}{g} \times \left[\frac{10^{-12}}{B(K_L^0 \rightarrow \mu e)} \right]^{1/4}. \quad (33)$$

Thus, upper limits in the range of 10^{-12} yield impressive lower bounds on M_X , at least if g_X is comparable to g . The following sections discuss the present experimental limits on LFV modes and the prospects for further improvement. While limits from rare kaon decays have provided the most stringent limits on some models of BSM physics, there are also strong limits from neutrino-less double beta decay and from several rare muon decays. The experimental focus in the field has now shifted to improving some of the rare muon decay limits.

4.1 $K_L^0 \rightarrow \mu e$

Experimental limits of $K_L^0 \rightarrow \mu e$ have steadily improved over the past decade [156-158] from a level of about 10^{-8} in 1988 to the final result of BNL E871 [159], published in 1998. The E871 spectrometer is described in Section 6.1.2. It features two analysis magnets for redundant momentum measurements. Electrons and muons are each identified in two different ways to reduce background from particle misidentification. The analysis cuts are then chosen to minimize the remaining backgrounds (involving either accidental coincidences or scattered electrons) while maintaining as much sensitivity as possible to the signal. The final cuts correspond to a single-event sensitivity of about 2×10^{-12} with an expected background of 0.1 event. The cuts are set without looking at the data within the exclusion box shown in Figure 14. This ‘‘blind’’ analysis technique ensures that the cut selection remains unbiased by the data, and it has been adopted in many of the rare decay analyses described in this article.

When the exclusion box is opened, no events are found in the smaller signal region. This allowed E871 to set a 90%-CL upper limit of $B(K_L^0 \rightarrow \mu e) < 4.7 \times 10^{-12}$, the smallest upper limit set to date on any kaon decay mode. For an exotic boson with electroweak coupling strength, Equation 30 then implies a lower bound on its mass of 150 TeV.

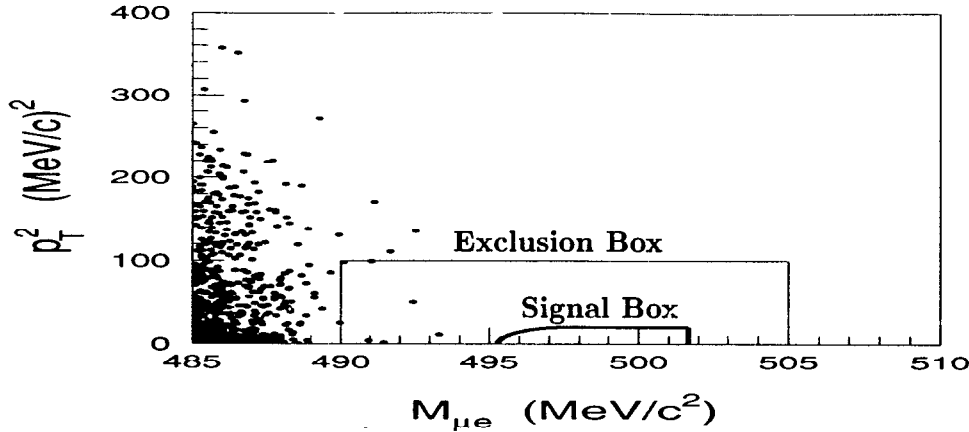


Figure 14: E871: Final data sample with the reconstructed mass $M_{\mu e}$ vs the square of the transverse momentum relative to the kaon direction, after all cuts there are no events in the signal region. The exclusion box (the larger box enclosing the signal box) was used to set cuts in an unbiased way on data far from the signal region. The shape of the signal box was optimized to maximize signal/background.

There are no near-term plans to pursue this decay further, as the background from $K_L^0 \rightarrow \pi^\pm e^\mp \nu_e$ with a muon decay and a scattered electron is difficult to reduce below a level of 10^{-13} , which is just beyond the E871 sensitivity.

4.2 $K^+ \rightarrow \pi^+ \mu^+ e^-$

E865 at BNL was designed to search for the LFV decay $K^+ \rightarrow \pi^+ \mu^+ e^-$. This decay, with an extra pion in the final state, is sensitive to exotic gauge bosons with different quantum numbers from those that E871 could detect. The experiment uses K^+ decays in flight, and the detector concept is similar to that of E871, with redundant particle identification by two Cerenkov detectors and an electromagnetic calorimeter, and a muon range stack (see Section 6.1.1). Data were collected during the 1995, 1996, and 1998 runs of the AGS. The limit on this mode from the 1995 run [160], similar in sensitivity to the predecessor experiment E777 [161], was $B(K^+ \rightarrow \pi^+ \mu^+ e^-) < 2.1 \times 10^{-10}$. The limit from the 1996 run [162], with no events above a likelihood to be $K^+ \rightarrow \pi^+ \mu^+ e^- (\mathcal{L}_{\pi\mu e})$ of 20%, is $B(K^+ \rightarrow \pi^+ \mu^+ e^-) < 3.9 \times 10^{-11}$ (see Figure 15). From the combined results from E777 and the E865 runs in 1995 and 1996, a limit of $B(K^+ \rightarrow \pi^+ \mu^+ e^-) < 2.8 \times 10^{-11}$ is obtained. The final sensitivity, with the 1998 data included, is expected to be ~ 3 times better. E865 is already close to being limited by background from accidentals; there are no plans to continue with this search. The E865 limit implies a lower bound of several tens of TeV on exotic bosons with electroweak coupling, depending on the exact model used.

4.3 $K_L^0 \rightarrow \pi^0 \mu e$

In addition to the search for $K^+ \rightarrow \pi^+ \mu^+ e^-$ performed by BNL E865, a search for the corresponding neutral mode $K_L^0 \rightarrow \pi^0 \mu e$ has been carried out by E799-I at FNAL (see Section 6.2.1). The main background concern was the common

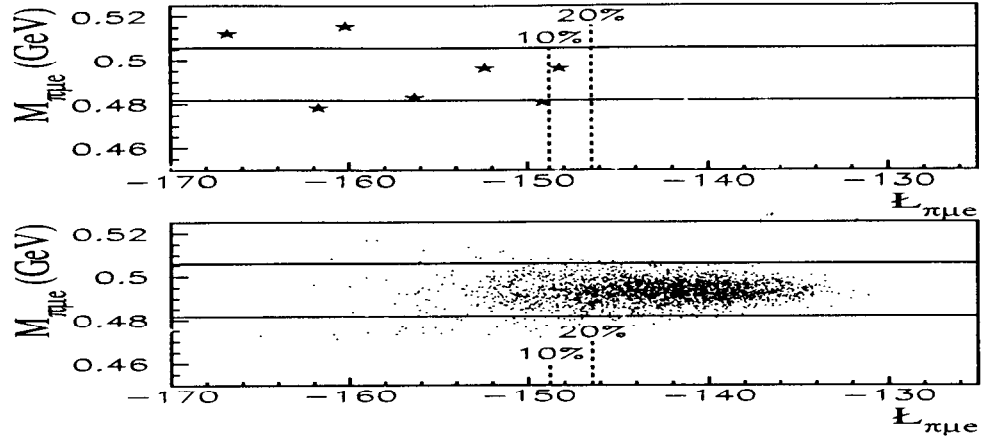


Figure 15: E865: Final 1996 data sample after all cuts, with no events above $\pi\mu e$ likelihood ($L_{\pi\mu e}$) of 20%. The $\pi\mu e$ likelihood is formed from the quality of the track fits, timing, vertex, reconstruction to the target, and particle identification. Also shown are $\pi\mu e$ Monte Carlo events passing all cuts.

decay $K_L^0 \rightarrow \pi^0 \pi^+ \pi^-$, in which one of the pions is misidentified as a muon and the other as an electron, or the rarer $K_L^0 \rightarrow \pi^\pm \pi^0 e^\mp \nu_e$ events with one misidentification. Both of these were efficiently eliminated by kinematic cuts. The remaining background from accidental coincidences is very small, as can be seen in Figure 16. The final 90%-CL limit² on $K_L^0 \rightarrow \pi^0 \mu e$ from E799-I [163] is $B(K_L^0 \rightarrow \pi^0 \mu e) < 3.1 \times 10^{-9}$. Given the low background level, it should be

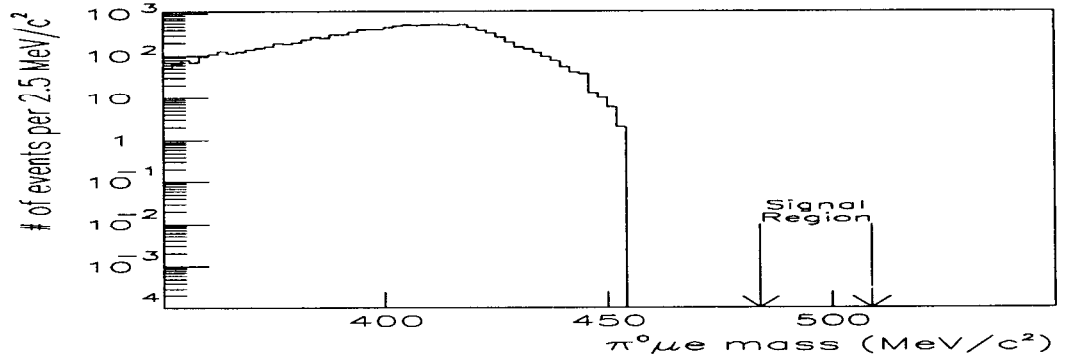


Figure 16: E799-I: Final 1986 data sample after all cuts, with no events above $M_{\pi\mu e} = 455 \text{ MeV}/c^2$.

possible for KTeV/E799-II to use its greater sensitivity to improve this limit by more than an order of magnitude, competitive with the charged-mode limit from E865.

4.4 Other Searches for New Physics

In addition to the LFV searches, there have been a number of other searches for BSM physics in recent years. These include $K^+ \rightarrow \pi^+ X^0$, $K^+ \rightarrow \pi^- \mu^+ \mu^+$, and $K^+ \rightarrow \pi^+ \mu^- e^+$. Table 11 summarizes BSM searches reported since the

²This limit is on the average of the two charge modes, not their sum.

previous review [1]. The E865 limit on $K^+ \rightarrow \pi^- \mu^+ \mu^+$ is derived from the

Table 11: Summary of searches for physics beyond the standard model

Decay Mode	Branching Ratio	Experiment
$K_L^0 \rightarrow \mu e$	$< 4.7 \times 10^{-12}$	E871 (1998) [159]
$K^+ \rightarrow \pi^+ \mu^+ e^-$	$< 2.8 \times 10^{-11}$	E865 (2000) [162]
$K_L^0 \rightarrow \pi^0 \mu e$	$< 3.1 \times 10^{-9}$	E799-I (1998) [163]
$K^+ \rightarrow \pi^+ X^0$	$< 1.1 \times 10^{-10}$	E787 (2000) [68]
$K^+ \rightarrow \pi^- \mu^+ \mu^+$	$< 3.0 \times 10^{-9}$	E865 (2000) [164]
$K^+ \rightarrow \pi^- e^+ e^+$	$< 6.4 \times 10^{-10}$	E865 (2000) [164]
$K^+ \rightarrow \pi^+ \mu^- e^+$	$< 5.2 \times 10^{-10}$	E865 (2000) [164]
$K^+ \rightarrow \pi^- \mu^+ e^+$	$< 5.0 \times 10^{-10}$	E865 (2000) [164]
$K_L^0 \rightarrow e^\pm e^\pm \mu^\mp \mu^\mp$	$< 6.1 \times 10^{-9}$	E799-I (1996) [165]

$K^+ \rightarrow \pi^+ \mu^+ \mu^-$ data set collected in 1997 and the other E865 lepton number violating limits in Table 11 derive from the $K^+ \rightarrow \pi^+ \pi^- e^+ \nu_e$ data set also collected in 1997. Existing KTeV data could be used to search for some other exotic modes, such as $K^0 \rightarrow \pi^\pm \pi^\pm e^\mp e^\mp$ and $K^0 \rightarrow \pi^\pm \pi^\pm \mu^\mp \mu^\mp$, in the near future.

5 CONCLUSIONS AND FUTURE PROSPECTS

The unprecedented sensitivities of the rare kaon decay experiments in setting limits on LFV have constrained many extensions of the standard model.

The observation of $K^+ \rightarrow \pi^+ \nu \bar{\nu}$ has opened the doors to measurements of the unitarity triangle completely within the kaon system. Significant progress in the determination of the fundamental CKM parameters will come from the generation of experiments that is starting now. Comparison with the B meson system will then overconstrain the unitarity triangle and test the standard-model explanation of CP violation.

The primary focus for the future of rare kaon decays is on the measurement of the golden modes, $K_L^0 \rightarrow \pi^0 \nu \bar{\nu}$ and $K^+ \rightarrow \pi^+ \nu \bar{\nu}$, at sensitivities sufficient for observation of 100 SM events. Major initiatives in this regard are underway at BNL, FNAL and KEK. At the same time the study of a number of medium-rare and radiative modes will be pursued, both as a by-product of the $K \rightarrow \pi \nu \bar{\nu}$ measurements and current ϵ'/ϵ measurements and in a dedicated study at IHEP.

5.1 Medium-Rare and Radiative Decays

The DAΦNE e^+e^- accelerator complex and KLOE detector at Frascati (Italy) (see Section 6.4) were both commissioned in 1999. It is expected that by the time the machine reaches the full luminosity of $5 \times 10^{32} \text{cm}^{-2} \text{s}^{-1}$, KLOE will be able to observe 10^{10} tagged kaons of all charges per year. In addition to the measurement of ϵ'/ϵ , KLOE will provide a wealth of new measurements on many rare and medium-rare decays, particularly for the K_S modes.

A new kaon decay experiment (see Section 6.5) is planned at the U70 accelerator in IHEP in Serpukhov. CERN has provided IHEP with an RF separator to be used in a 12-GeV/c separated kaon beam. This experiment may have even greater sensitivity than KLOE to medium-rare charged kaon decays.

The NA48 collaboration has planned a special run after the final ϵ'/ϵ running, with the K_L beam turned off, dedicated to improving sensitivity to rare K_S decays. NA48 is also considering improved measurements of some charged kaon decays.

5.2 $K \rightarrow \pi \nu \bar{\nu}$

The principal focus of the kaon community is the precise measurement of the $K \rightarrow \pi \nu \bar{\nu}$ decay modes. These measurements will provide critical, unambiguous determination of the standard-model CP violation parameters. Comparison with measurements from the B meson system will then over-constrain these parameters and test the standard-model picture of CP violation.

These measurements are difficult, but several clear and convincing cases have been made for measuring up to $\mathcal{O}(100)$ events in both modes. This is as far as it makes sense to go with measurements of $K^+ \rightarrow \pi^+ \nu \bar{\nu}$, as the charm quark uncertainty in extracting $|V_{td}|$ will then dominate. In $K_L^0 \rightarrow \pi^0 \nu \bar{\nu}$, experimental uncertainties will dominate the errors.

5.2.1 $K^+ \rightarrow \pi^+ \nu \bar{\nu}$

A clean, convincing $K^+ \rightarrow \pi^+ \nu \bar{\nu}$ event has already been seen by E787. Building on this success, the new E949 experiment will make modest and well-understood upgrades to the E787 detector, which has already demonstrated sufficient background rejection for a very precise measurement of $B(K^+ \rightarrow \pi^+ \nu \bar{\nu})$. The experiment will make use of the entire proton flux from the AGS to increase its sensitivity per hour by a factor of 15 over the sensitivity E787 achieved in 1995. E949 is currently under construction and will run in 2001 through 2003. The E949 sensitivity should reach one order of magnitude below the expectation for the signal, and the experiment should observe 10 standard-model events. The background is well-understood and is 10% of the standard-model signal.

A proposal to improve the $K^+ \rightarrow \pi^+ \nu \bar{\nu}$ sensitivity by a further factor of ten has been initiated at FNAL. The CKM experiment plans to collect 100 standard-model events, with a background to signal ratio of $\sim 10\%$, in a two-year run starting about 2005. This experiment will use a new technique, with K^+ decay-in-flight and momentum/velocity spectrometers. It will have significant muon veto and photon veto capabilities and redundant tracking of both the kaon and pion.

5.2.2 $K_L^0 \rightarrow \pi^0 \nu \bar{\nu}$

The next generation of $K_L^0 \rightarrow \pi^0 \nu \bar{\nu}$ experiments will start with E391a at KEK, which hopes to reach a sensitivity of $\sim 10^{-10}$. Although the reach of E391a is not sufficient to observe a signal at the standard model level the experiment will be able to rule out large BSM enhancements and learn more about how to do this difficult experiment. It is designed around a pencil K_L beam, a high-resolution crystal calorimeter, and very efficient photon veto systems. This experiment would eventually move to the JHF and aim for a sensitivity of $\mathcal{O}(10^{-14})$.

KAMI plans to reuse the excellent KTeV CsI calorimeter, which will have to be restacked to accommodate the single KAMI beam. The decay volume upstream of the calorimeter will be instrumented with a fiber-tracker system and surrounded

by a hermetic, highly efficient array of photon veto detectors. An additional photon detector will catch photons escaping along the beam. The initial KAMI run (the KAMI-far configuration) would take place with the target in the same location as for KTeV, some 180 m upstream of the CsI calorimeter. Later, the target would be moved downstream (the KAMI-near configuration) in order to increase the solid angle and the resulting kaon intensity. KAMI hopes to collect about 20 events per year of running in the KAMI-far configuration, increasing to 100 events per year with KAMI-near. Backgrounds due to lost photons are a major concern, particularly due to photons escaping down the beam hole, where there is a high neutron flux. If KAMI is approved, running in the KAMI-far configuration may begin around 2005–2006, with KAMI-near following perhaps around 2008.

KOPIO follows a different strategy. The kaon center of mass will be reconstructed using a bunched proton beam and a very-low-momentum K_L beam. This technique allows for two independent criteria to reject background, photon veto and kinematics—allowing background levels to be directly measured from the data—and encourages further confidence in the signal by measuring the momentum spectrum of the decay. A large flux will be obtained using the entire AGS proton current. The low-energy beam also substantially reduces backgrounds from neutrons and other sources. After three years of running, 65 standard-model events are expected with a $S/B \geq 2:1$.

6 EXPERIMENTAL CONFIGURATIONS

6.1 BNL: AGS

The Alternating Gradient Synchrotron (AGS) at Brookhaven National Laboratory (BNL) began operation in 1960. In the intervening 40 years, the intensity has increased substantially to ≥ 65 Tp (Tp $\equiv 10^{12}$ protons per spill). The typical cycle time of the accelerator up to 1990 was a 1-s spill every 3 s (33% duty factor). Since that time, the duty factor has been increased as high as 55% (in 1998), with a 2.8-s spill every 5.1 s. The AGS has also achieved microbunching during extraction, as required by the proposed E926 $K_L^0 \rightarrow \pi^0 \nu \bar{\nu}$ experiment.

6.1.1 E865

Experiment E777, a search for $K^+ \rightarrow \pi^+ \mu^+ e^-$ [101,161], ran from 1986 through 1988 and was then modified slightly, E851, to optimize for $\pi^0 \rightarrow e^+ e^-$ from $K^+ \rightarrow \pi^+ \pi^0$ [166] and $K^+ \rightarrow \pi^+ e^+ e^-$ [102] and ran in 1989. An upgraded experiment, E865 [167] (see Figure 17), to search for $K^+ \rightarrow \pi^+ \mu^+ e^-$ [103,105,160,162] ran from 1995 through 1998. The detector sits in an intense unseparated 6-GeV/c K^+ beam, with 30 MHz of K^+ and 600 MHz of π^+ . The first magnet separates the charged kaon decay products, with negative particles going left; the second magnet provides momentum analysis of these tracks with four stations of high-rate multi-wire proportional chambers. Particle identification consists of two sets of segmented threshold Cerenkov counters: the left side, with a high threshold gas (H_2), was optimized to reject μ 's and π 's; the right side, with a low threshold gas (CO_2 or CH_4), was optimized to reject e^+ from π^0 Dalitz decays. In addition, a Pb-scintillator Shashlyk calorimeter provides electron identification and a range stack of alternating iron plates and multi-wire proportional chambers provides

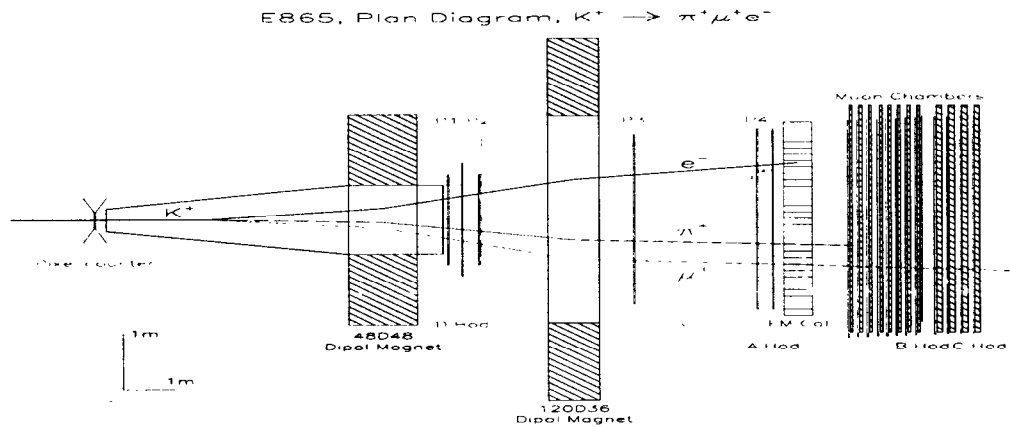


Figure 17: Plan view of the E865 detector at BNL.

muon identification.

6.1.2 E871

Experiment E791 [168], a search for $K_L^0 \rightarrow \mu e$ [157,169], ran from 1988 through 1990. An upgraded experiment to continue the $K_L^0 \rightarrow \mu e$ [49,50,159] search, E871 [170], ran during 1995–1996 (see Figure 18). The spectrometer has two

BNL Experiment 871 - The Search for $K_L^0 \rightarrow \mu e$

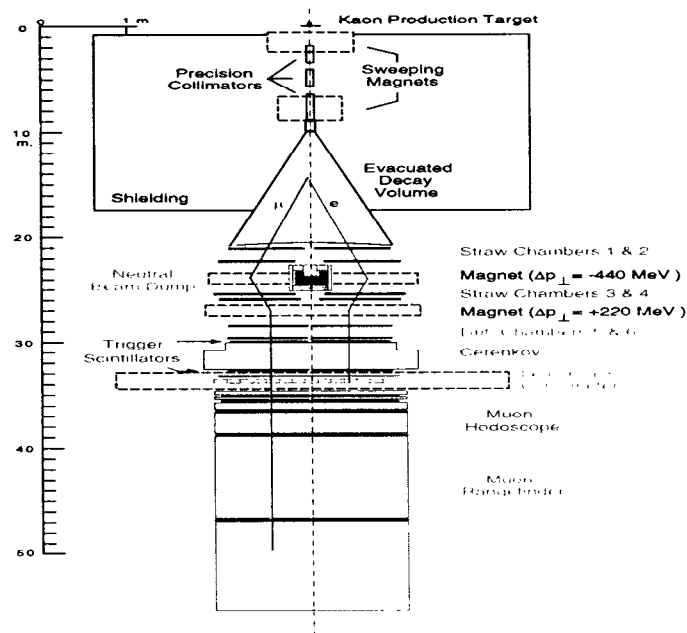


Figure 18: Plan view of the E871 detector at BNL.

arms, each with six gas-drift tracking stations and two momentum-analyzing magnets to provide independent momentum measurements. Each tracking station has three x (bending plane) measurements to minimize the probability of

tracking errors. This is critical, as a tracking mistake in combination with a pion decay can give a good track χ^2 with a mismeasured momentum. A novel beam plug, to stop the neutral beam in the center of the first magnet, succeeded in reducing rates in the downstream particle identification detectors. Redundant electron identification uses an H₂ Cerenkov counter and a lead glass calorimeter. Muon identification is achieved with a range stack of scintillator and drift tubes with an absorber of iron, marble and aluminum.

6.1.3 E787 & E949

Experiment E787 [171], to search for $K^+ \rightarrow \pi^+ \nu \bar{\nu}$ (see Figure 19), ran from 1989 through 1991 [67,96,104,172] and again, after an upgrade [173], from 1994 through 1998 [68,126]. The E787 detector is located in a low-energy separated K^+ beam.

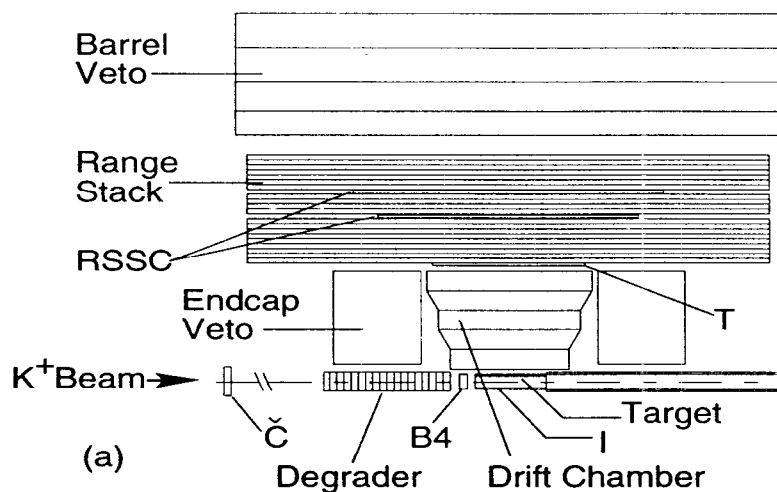


Figure 19: Elevation view of the top half of the E787 detector at BNL.

The beam particles are tagged with a Cerenkov counter and tracked with MWPC and scintillator counters until stopped in a scintillating fiber target inside of a 1-T magnetic field. The kaon decay particles are tracked through the fiber target, a low-mass central drift chamber, and into a segmented cylindrical plastic scintillator range stack, with embedded straw tube chambers. The $\pi^+ \rightarrow \mu^+ \rightarrow e^+$ decay chain is identified with 500-MHz transient digitizers recording output from the entire range stack. The detector is surrounded by a nearly hermetic photon veto system.

The E949 experiment (see Figure 20), upgrading the E787 detector, will run from 2001 through 2003. The E949 detector will increase photon veto coverage with an additional Pb-scintillator barrel veto liner and additional photon veto coverage along the beam axis. Part of the range stack scintillator will be replaced to obtain more light, and several non- or poorly working detectors will be replaced. The trigger and DAQ systems will be substantially upgraded.

6.1.4 KOPIO/E926

Experiment E926, named KOPIO, (see Figure 21) received scientific approval at BNL in 1997 but is not yet funded. Its proponents, together with those from the competing FNAL proposal called KAMI (see below), are undertaking joint

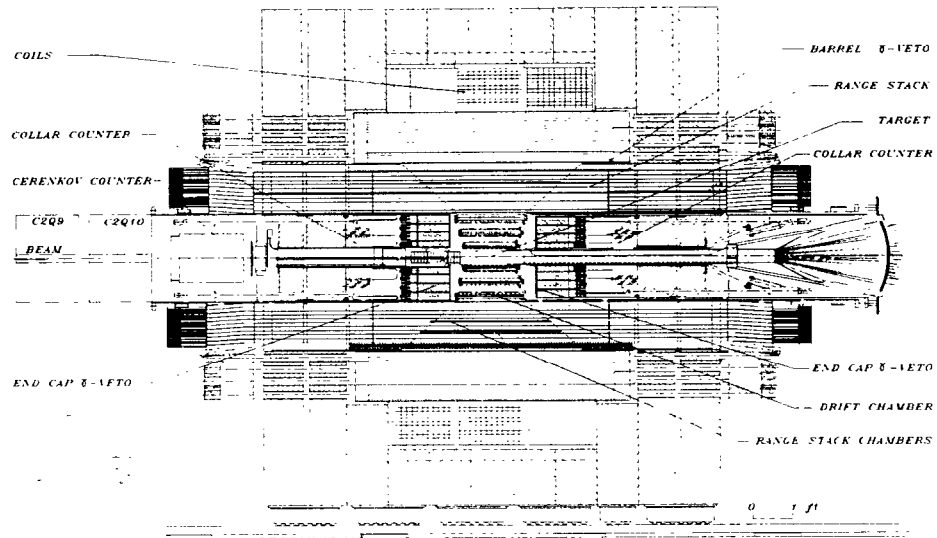


Figure 20: Elevation view of the E949 detector at BNL.

research and development efforts with the aim of identifying the best technique for a future $K_L^0 \rightarrow \pi^0 \nu \bar{\nu}$ measurement. In the proposed KOPIO experiment, the

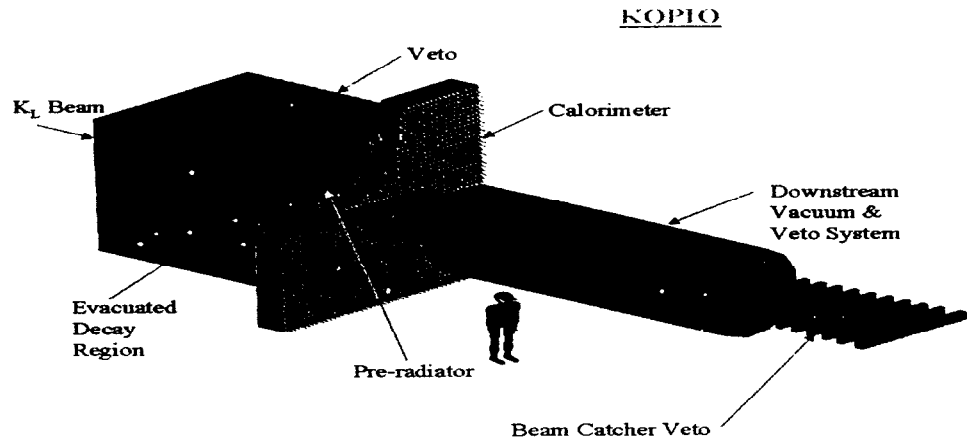


Figure 21: The Proposed KOPIO detector at BNL.

AGS proton beam is micro-bunched, with 200-ps bunches every 40 ns. The angle of the neutral kaon beam is 45° , with an average K_L momentum of 700 MeV/c. The kaon time of flight is used to measure the kaon momentum and the decay π^0 momentum in the kaon center-of-mass frame. The neutrons at this large targeting angle are mostly below π^0 production threshold. The beam is very well collimated and flat. The detector consists of a Shashlyk calorimeter and a pre-radiator of scintillator and copper drift chambers. The vacuum decay volume is surrounded by a charged particle veto and a very thin vacuum tank. The outside of the tank is surrounded by Pb-scintillator photon veto. A Pb-aerogel Cerenkov detector

will be mounted in the beam hole for additional photon veto.

6.2 FNAL: Tevatron, Main Injector

The Tevatron at FNAL began operation in 1984. The typical proton intensity delivered to kaon experiments ranged from 7×10^{11} protons per 20-s spill (60-s duty cycle) for E731, the ϵ'/ϵ experiment that collected data in 1987–1988, to as high as 10 Tp per 40-s spill (80-s duty cycle) during the 1999–2000 run of the rare decay experiment E799-II. The Main Injector was commissioned in 1999 and was used as an injector to the Tevatron during the 1999–2000 run. Future fixed-target experiments are proposed to run with a 120-GeV/c beam directly from the Main Injector while the collider is running. The Main Injector can supply 30 Tp per 3-s spill, allowing experiments to run at much greater intensity than is possible at the Tevatron.

6.2.1 KTeV

Experiment E799-I ran during 1991 and early 1992, during the same fixed-target run as the CP -violation experiment E773, which used the same detector. The primary goal of E799-I was to search for $K_L^0 \rightarrow \pi^0 e^+ e^-$ and $K_L^0 \rightarrow \pi^0 \mu^+ \mu^-$, but a variety of other rare decays were studied [56,58,81,110,143,163,165,174], including $K_L^0 \rightarrow e^+ e^- e^+ e^-$, $K_L^0 \rightarrow \mu^+ \mu^- e^+ e^-$ and $K_L^0 \rightarrow \pi^0 \mu e$. The single-event sensitivity achieved for four-body modes was in the range of 10^{-9} .

The KTeV proposal consists of two experiments: E832, a precision measurement of $Re(\epsilon'/\epsilon)$, and E799-II, a second, upgraded phase of the earlier E799-I, which had been envisioned in the original E799 proposal. The centerpiece of the KTeV detector is a large, high-precision CsI calorimeter [175] capable of measuring photon and electron energies to better than 1% precision. The new detector reuses the drift chambers from E799-I, but everything else is new, including an extensive transition radiation detector (TRD) system for enhanced pion-electron separation, a greatly upgraded array of photon veto detectors, and a trigger and data acquisition system with about 50 times the bandwidth of the one used in E799-I.

E799-II (see Figure 22) collected data during fixed target runs in 1996–1997 and 1999–2000. A number of results from the analysis of the data from the first run have been published or reported at conferences [70,71,90,119,121]. Data from the 1999–2000 run will increase the experiment's rare kaon decay sensitivity by a factor of two to three, depending on the mode. With the complete data set, E799-II should achieve an improvement of about a factor of 20 over E799-I in single-event sensitivity for $K_L^0 \rightarrow \pi^0 e^+ e^-$ and $K_L^0 \rightarrow \pi^0 \mu^+ \mu^-$.

6.2.2 KAMI/E804

KAMI (Kaons At the Main Injector) is the name of the detector proposed in FNAL Expression of Interest 804 (see Figure 23). As presently conceived, KAMI focuses on the difficult but rewarding mode $K_L^0 \rightarrow \pi^0 \nu \bar{\nu}$. It competes with the proposed KOPIO experiment at BNL (see above). The KAMI proposal includes reusing the high-resolution KTeV CsI calorimeter but replaces the tracking and photon veto systems. In order to achieve the very high background rejection needed to see a $K_L^0 \rightarrow \pi^0 \nu \bar{\nu}$ signal at the standard-model level, KAMI uses a

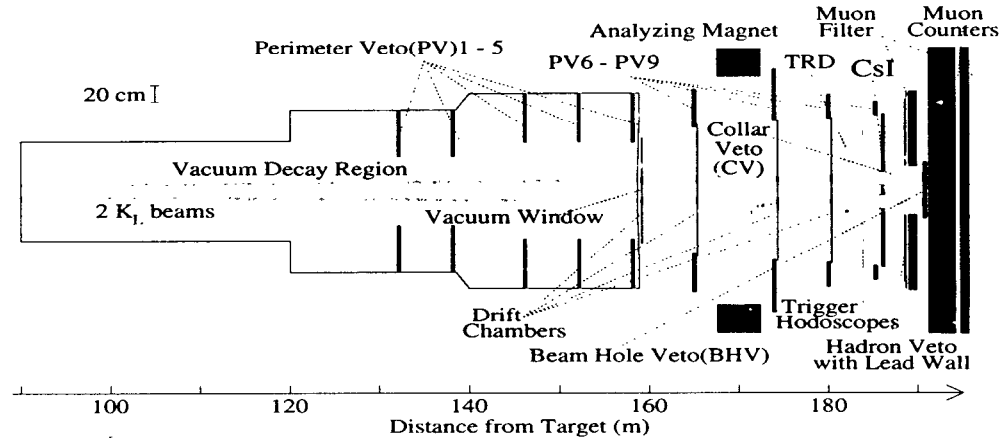


Figure 22: Plan view of the KTeV detector at the Tevatron at FNAL.

completely hermetic photon veto system with good photon detection efficiency down to energies as low as 20 MeV at large angles. A major challenge for KAMI is the design of a beam-hole photon detector that would function in the presence of a very large neutron flux. KAMI also plans to continue the study of $K_L^0 \rightarrow \pi^0 e^+ e^-$ and $K_L^0 \rightarrow \pi^0 \mu^+ \mu^-$, as well as other rare kaon decays, by building a system of fiber trackers. KAMI is not yet approved, but hopes to collect data beginning about 2005.

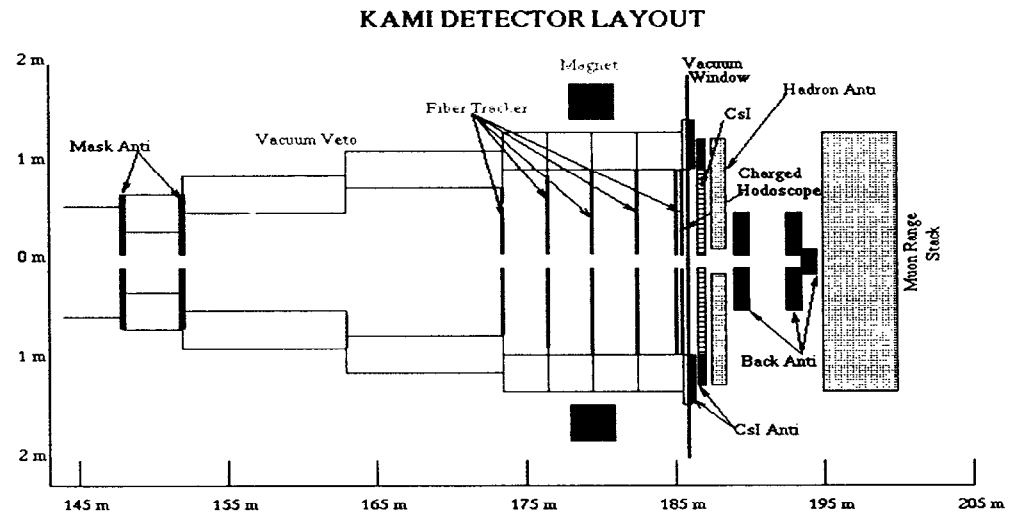


Figure 23: Plan view of the proposed KAMI detector at FNAL.

6.2.3 CKM/E905

The CKM (Charged Kaons at the Main injector) experiment (see Figure 24) is proposed to run at the Main Injector at FNAL. In the proposed experiment, a 22-GeV/c separated K^+ beam, with $K/\pi = 2:1$, and 30 MHz of K^+ decays are delivered to the detector. A debunched proton beam of 5 Tp is ex-

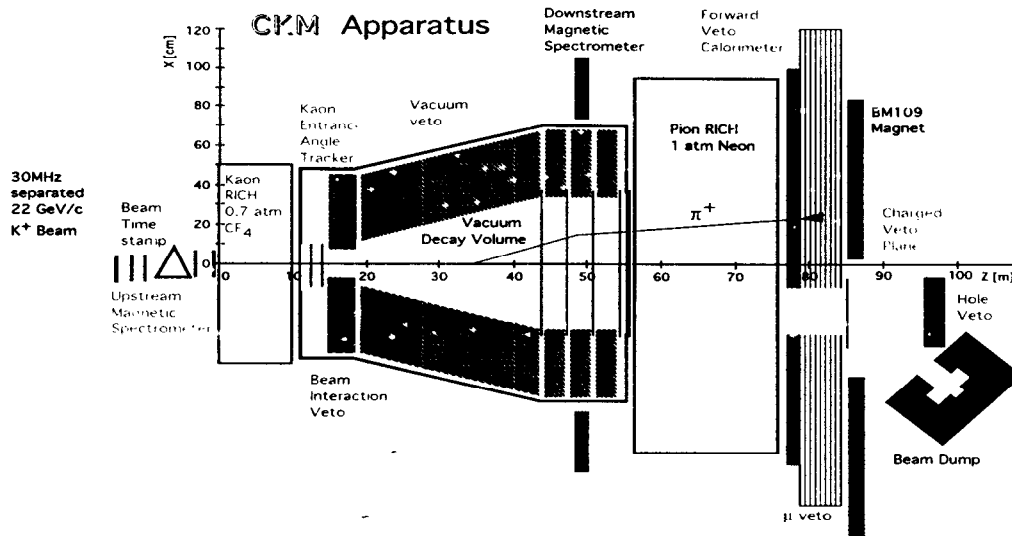


Figure 24: Plan view of the proposed CKM detector at FNAL.

tracted from the Main Injector with high duty factor. The incident K^+ beam is momentum-analyzed in a Si-tracking system before impinging on a kaon ring imaging Cerenkov hodoscope (RICH), where its velocity and direction are re-measured. The K^+ direction is measured a final time inside the vacuum decay volume; then the decay π^+ is momentum-analyzed and tracked with low-mass straw tube chambers in the vacuum. A pion RICH measures the π^+ velocity and direction. A muon veto system establishes that the outgoing track was a π^+ . The entire apparatus is surrounded by photon veto systems.

6.3 NA48

The CERN Super Proton Synchrotron provides extracted protons at 400-GeV/c for a fixed target program including the rare kaon decay experiments NA31 and its successor, NA48. The NA31 experiment [176], designed to measure ϵ'/ϵ , also searched for rare K_L and K_S decays [53,77,82,123,153,177] from 1982 through 1991. An upgraded experiment, NA48 [178], again with the primary aim to measure ϵ'/ϵ will measure several rare decays [80,150,179] as well (see Figure 25). The NA48 beamline is innovative in its use of a bent crystal to deflect a small fraction of the proton beam onto a K_S target just upstream of the spectrometer. This provides the opportunity to study rare K_S decays. The centerpiece of the NA48 detector is a high-precision liquid krypton calorimeter of unprecedented size. Energy resolutions of better than 1% for photons and electrons have been achieved with this device, which was completed in 1997. NA48 had an engineering run in 1996 and data-taking runs in 1997–1999. Unfortunately, on November 15, 1999, the vacuum pipe for the beam traversing the center of the spectrometer imploded, destroying the drift chamber spectrometer. Current plans are for a short run in 2000 to search for $K_S^0 \rightarrow \pi^0 \pi^0 \pi^0$ and further running with the rebuilt spectrometer starting in 2001.

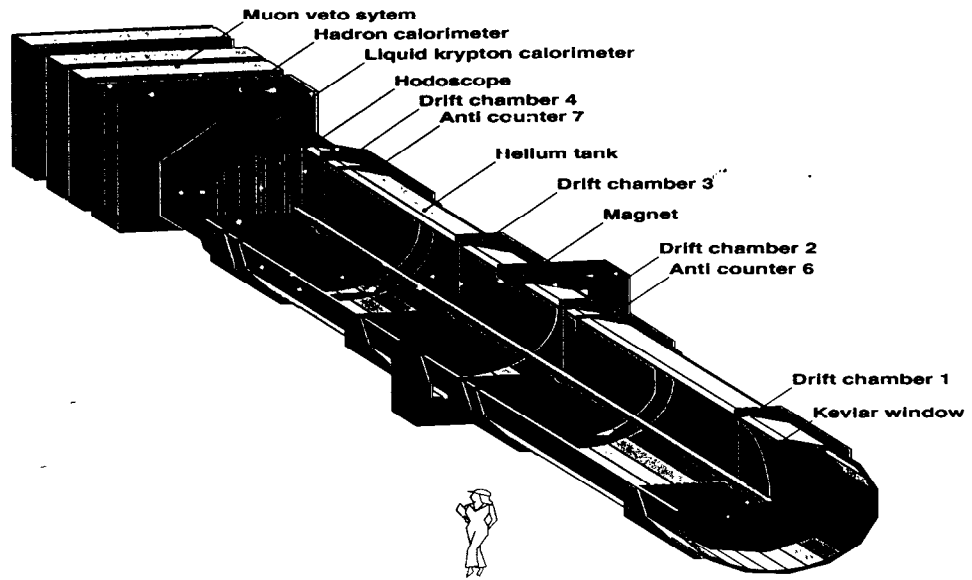


Figure 25: The NA48 detector at CERN.

6.4 KLOE

The DAΦNE Φ factory in Frascati, is a 1.02-GeV e^+e^- collider sitting at the Φ peak. The accelerator began commissioning in early 1999, with a design luminosity goal of $L = 5 \times 10^{32}$.

The KLOE experiment [180] was designed to measure ϵ'/ϵ , although it will search for a variety of rare K_L , K_S and K^+ decays (see Figure 26) with tagged

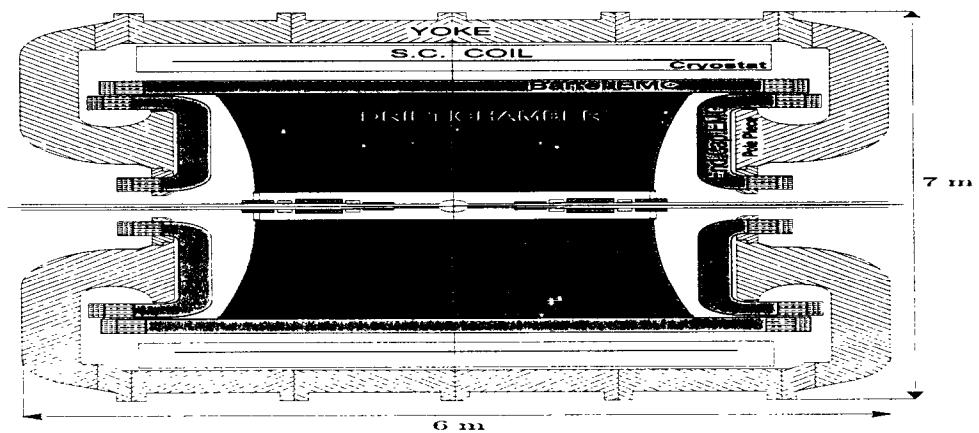


Figure 26: Elevation view of the KLOE detector at Frascati.

kaons from copious Φ decays. At the DAΦNE e^+e^- collider KLOE is working in the center of mass frame. It is a cylindrically symmetric general-purpose detector with a low-mass central drift chamber of very large volume (4-m diameter),

surrounded by a Pb-scintillating fiber calorimeter. The detector is in a 0.6-T magnetic field, so the calorimeter is read out with high-field fine-mesh PMTs.

6.5 IHEP: Separated Kaon Experiment

The U-70 accelerator at IHEP in Serpukhov has reached an intensity of 15 Tp. It runs with a 2-s spill every 10 s, for a duty factor of 20%.

A new experiment at IHEP is proposed to run in the N-21 line with a 12-GeV/c separated K^\pm beam starting in 2002. This experiment will study a variety of medium-rare (mostly radiative) kaon decays and should be able to substantially improve existing measurements. This experiment will use a new RF separator from CERN [181] to provide a K purity of 2:1. The experiment will reuse existing apparatus from SPHINX, GAMS, and ISTRAM.

6.6 KEK

The Proton Synchrotron (PS) at KEK in Japan can deliver up to 6 Tp during a 0.7-s spill every 3 s. During the past 15 years several experiments have been operating in high intensity kaon beams, starting with E137, E162 and now with E391a.

Experiment E137, the first K_L decay experiment at the KEK PS searched for the decay $K_L^0 \rightarrow \mu e$ [158] from 1988 through 1990. In addition to the search for $K_L^0 \rightarrow \mu e$, E137 set limits on $K_L^0 \rightarrow e^+e^-$ and measured branching ratios for $K_L^0 \rightarrow \mu^+\mu^-$ [158,182] and $K_L^0 \rightarrow e^+e^-e^+e^-$ [183]. The experiment ran with 2 Tp of protons on target and $\sim 10^7$ K_L per spill. The neutral-beam solid angle was $154 \mu\text{str}$ at production angles of 0° and 2° . The E137 detector consisted of a two-arm spectrometer with five drift chamber stations and two dipole magnets, with a total P_T of 238 MeV/c, in each arm. Particle identification consisted of threshold gas Cerenkov counters, a Pb-scintillator electromagnetic calorimeter, and a muon range stack.

Experiment E162 was designed to search for $K_L^0 \rightarrow \pi^0 e^+ e^-$ (see Figure 27). After an engineering run that indicated that neutron contamination in the beam was too high, the experiment changed focus to search for $K_L^0 \rightarrow \pi^+ \pi^- e^+ e^-$ [184] and collected data from 1996 through 1997. In addition to $K_L^0 \rightarrow \pi^+ \pi^- e^+ e^-$, a limit on $K_L^0 \rightarrow \pi^0 e^+ e^- \gamma$ [185] was set.

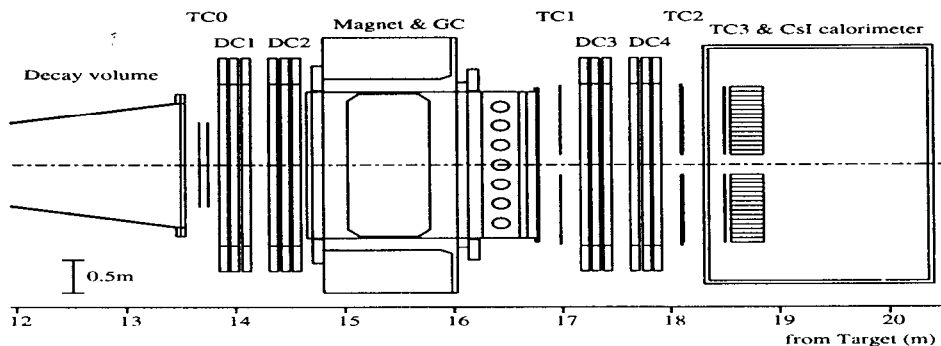


Figure 27: Plan view of the E162 detector at KEK.

Experiment E162 ran with a neutral kaon beam of $8 \text{ mrad} \times 20 \text{ mrad}$ at a production angle of 2° and 1 Tp of protons on target in a 2-s spill every 4 s. The spectrometer consisted of four drift chambers (x , u and v) views and a magnet with $136 \text{ MeV}/c$ P_T kick. Particle identification included a threshold gas Cerenkov counter and an undoped CsI calorimeter.

Experiment E391a will search for $K_L^0 \rightarrow \pi^0 \nu \bar{\nu}$ (see Figure 28). It is scheduled to run at the KEK PS from 2001 through 2005. The detector has a high-resolution

E391a Detector Plan

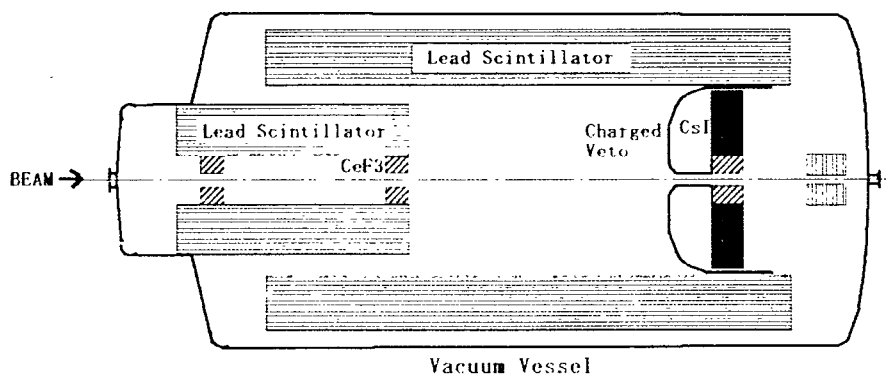


Figure 28: Plan view of the E391a detector at KEK.

crystal calorimeter and is otherwise surrounded by Pb-scintillator photon veto. The entire detector is situated in vacuum. The pencil beam is incident on the detector, giving a very small solid angle for background with a photon going down the beam hole. There is a plan to move this experiment to the JHF and, with the increased flux, measure $\mathcal{O}(1000)$ events.

7 Acknowledgments

We would like to thank the many people who helped with this paper by providing data and useful comments. We would particularly like to acknowledge Laurie Littenberg, Yau Wah, Hong Ma, Stefan Pislak, Robin Appel, Jim Lowe, Mike Zeller, Bill Molzon, Toshio Numao, Takao Inagaki, Takeshi Komatsubara, Tadashi Nomura, Leonid Landsberg, Brad Cox, Breese Quinn, and Yoshi Kuno. This work was supported in part under US Department of Energy contract #DE-AC02-98CH10886.

Literature Cited

1. Littenberg L, Valencia G. *Annu. Rev. Nucl. Part. Sci.* 43:729 (1993)
2. Hagelin J, Littenberg L. *Prog. Part. Nucl. Phys.* 23:1 (1989); Ritchie J, Wojcicki S. *Rev. Mod. Phys.* 65:1149 (1993); Buchholz P, Renk B. *Prog. Part. Nucl. Phys.* 39:253 (1997)
3. Buchalla G, Buras AJ, Lautenbacher ME. *Rev. Mod. Phys.* 68:1125 (1996)
4. Buras AJ, Fleischer R. In *Heavy Flavours II*, ed. AJ Buras, M Lindner, pp. 65 Singapore: World Sci. (1997); also hep-ph/9704376
5. Buras AJ. In *Probing the Standard Model of Particle Interactions*, ed. Gupta R, De Rafael E, David F, Morel A, Vol. I, Ch. 5, New York, Elsevier Sci. (1999); also hep-ph/9806471
6. D'Ambrosio G, Isidori G. *Int. J. Mod. Phys.* A13:1 (1998)

7. Winstein B, Wolfenstein L. *Rev. Mod. Phys.* 65:1113 (1993)
8. Christenson JH, Cronin JW, Fitch VL, Turlay R. *Phys. Rev. Lett.* 13:138 (1964)
9. Alavi-Harati A, et al. *Phys. Rev. Lett.* 83:22 (1999)
10. Fanti V, et al. *Phys. Lett.* B465:335 (1999); Graziani G, In Ref. [30]
11. Brown R, et al. *Nature* 163:82 (1949)
12. Pais A. *Phys. Rev.* 86:663 (1952); Gell-Mann M. *Phys. Rev.* 92:833 (1953)
13. Dalitz R. *Phys. Rev.* 94:1046 (1954)
14. Lee TD, Yang CN. *Phys. Rev.* 104:254 (1956)
15. Cabibbo N. *Phys. Rev. Lett.* 10:531 (1963)
16. Kobayashi M, Maskawa T. *Prog. Theor. Phys.* 46:652 (1973)
17. Glashow SL, Iliopoulos J, Maiani L. *Phys. Rev. D* 2:1285 (1970)
18. Gaillard MK, Lee BW. *Phys. Rev. D* 10:397 (1974)
19. A. Astbury, et al., eds. *Proc. XXIX Int. Conf. High Energy Phys., Vancouver, Canada, July 1998* Singapore: World Sci. (1999)
20. Arisaka K and Bern Z, eds. *Proc. Meet. DPF, UCLA, Jan. 1999.* <http://www.dpf99.library.ucla.edu> (1999)
21. J. Tran Thanh Van, ed. *Proc. XXXIV Rencontres de Moriond, Les Arcs, France, March 1999* Paris: Ed. Frontieres (1999)
22. Földt G, et al., eds. *Proc. XVth Particles and Nuclei Int. Conf., Uppsala, Sweden, June 1999* Singapore: World Sci. (2000)
23. Huitu K, et al., eds. *Proc. Int. Europhys. Conf. High Energy Phys., Tampere, Finland, July 1999* Bristol, UK: IOP-Publishing
24. Rosner JL and Winstein B, eds. *Kaon Physics*, Proc. Chicago Conf. Kaon Phys., June 1999 Chicago: Univ. Chicago Press (2000)
25. Dauncey P and Sachrajda C, eds. *Proc. Heavy Flavours 8, Southampton, UK, July 1999* Southampton: J. High Energy Phys. (1999) <http://jhep.sissa.it/cgi-bin/PrHEP/cgi/reader/list.cgi?confid=3>
26. Jaros J and Peskin M, eds. *Proc. XIX Int. Symp. Lepton and Photon Interact. at High Energies, Stanford, August 1999.* Singapore: World Sci. (2000)
27. Capon G, et al., eds. *Proc. 3rd DAΦNE Workshop Phys. and Detectors, Frascati, Italy, Nov. 1999* Frascati Phys. Ser. Frascati: INFN Laboratori Nazionali di Frascati (2000)
28. Cheng HY and Hou WS, eds. *Proc. 3rd Int. Conf. B Phys. and CP Violation, Taipei, Taiwan, Dec. 1999* Singapore: World Sci. (2000)
29. Bellettini G, Chiarelli G, Greco M, eds. *Proc. 14th Workshop in Part. Phys., La Thuile, Italy, Feb. 2000* Frascati: INFN Laboratori Nazionali di Frascati (2000)
30. J. Tran Thanh Van, ed. *Proc. XXXV Rencontres de Moriond, Les Arcs, France, March 2000* Paris: Ed. Frontieres (2000)
31. *Proc. XXX Int. Conf. High Energy Phys., Osaka, Japan, July 2000* Singapore: World Sci. (2001)
32. Wolfenstein L. *Phys. Rev. Lett.* 51:1945 (1983)
33. Buras AJ, Lautenbacher ME, Ostermaier G. *Phys. Rev. D* 50:3433 (1994)
34. Jarlskog C. *Phys. Rev. Lett.* 55:1039 (1985); Jarlskog C. *Z. Phys. C* 29:491 (1985); Jarlskog C and Stora R. *Phys. Lett.* B208:268 (1988)
35. Marciano WJ. In Ref. [24] (2000)
36. Weinberg S. *Physica* A96:327 (1979); Gasser J, Leutwyler H. *Nucl. Phys.* B250:465 (1985); Leutwyler H. *Ann. Phys.* 235:165 (1994)
37. Gasser J, Leutwyler H. *Ann. Phys.* 158:142 (1984)
38. Leutwyler H, Roos M. *Z. Phys. C* 25:91 (1984)
39. Caso C, et al. *Euro. Phys. J.* C3:1. <http://pdg.lbl.gov> (1998)
40. Rosner JL. In *Proc. 2nd Tropical Workshop in Part. Phys. and Cosm., San Juan, Puerto Rico, May 2000* New York: AIP (2001)
41. Bargiotti M, et al. *Riv. Nuov. Cim.* In press (2000); also hep-ph/0001293 (2000) and references therein; Caravaglios F, Parodi F, Roudeau P, Stocchi A. In Ref. [28] (2000)
42. Sehgal LM. *Phys. Rev.* 183:1511 (1969)
43. D'Ambrosio G, Isidori G, Portolés J. *Phys. Lett.* B423:385 (1998)
44. Gómez Dumm D, Pich A. *Phys. Rev. Lett.* 80:4633 (1998)
45. Valencia G. *Nucl. Phys.* B517:339 (1998)
46. Knecht M, Peris S, Perrottet M, de Rafael E. *Phys. Rev. Lett.* 83:5230 (1999)
47. Geng CQ, Ng JN. *Phys. Rev. D* 41:2351 (1990)

48. Inami T, Lim CS. *Prog. Theor. Phys.* 65:297 (1981)
49. Ambrose D, et al. *Phys. Rev. Lett.* 84:1389 (2000)
50. Ambrose D, et al. *Phys. Rev. Lett.* 81:4309 (1998)
51. Donoghue JF, Gabbiani F. *Phys. Rev. D* 51:2187 (1995)
52. Bosch S, et al. *Nucl. Phys.* B565:3 (2000)
53. Barr GD, et al. *Phys. Lett.* B304:381 (1993)
54. Greenlee HB. *Phys. Rev. D* 42:3724 (1990)
55. Yamanaka T. In Ref. [21] (1999)
56. Barker A, et al. *Phys. Rev. D* 41:3546 (1990)
57. Ohl KE, et al. *Phys. Rev. Lett.* 64:2755 (1990)
58. Harris DA, et al. *Phys. Rev. Lett.* 71:3918 (1993)
59. Alavi-Harati A, et al. *Phys. Rev. Lett.* 84:5279 (2000)
60. Buchalla G, Buras A. *Nucl. Phys.* B412:106 (1994)
61. Marciano WJ, Parsa Z. *Phys. Rev. D* 53:R1 (1996)
62. Buchalla G, Buras A. *Phys. Rev. D* 57:216 (1998)
63. Buchalla G, Buras A. *Nucl. Phys.* B548:309 (1999)
64. Willocq S. In Ref. [28] (2000); also www.cern.ch/LEPBOSC
65. Buras AJ, et al. *Nucl. Phys.* B566:3 (2000) and references therein
66. Pallante E, Pich A, *Phys. Rev. Lett.* 84:2568; Buras AJ, In Ref. [24]; Buras AJ, et al. *Nucl. Phys.* B408:209 (1993); Bertolini S, Eeg JO, Fabbrichesi M, Lashin EI. *Nucl. Phys.* B514:93 (1998)
67. Adler S, et al. *Phys. Rev. Lett.* 79:2204 (1997)
68. Adler S, et al. *Phys. Rev. Lett.* 84:3768 (2000); Kettell SH. In Ref. [28]
69. Grossman Y, Nir Y. *Phys. Lett.* B398:163 (1997)
70. Adams J, et al. *Phys. Lett.* B447:240 (1999)
71. Alavi-Harati A, et al. *Phys. Rev. D* 61:072006 (2000)
72. Geng CQ, Hsu IJ, Lin YC. *Phys. Rev. D* 50:5744 (1994); Littenberg LS, Valencia G. *Phys. Lett.* B385:379 (1996)
73. Ng C. *The Search for the Rare Decay of $K^+ \rightarrow \pi^+ \pi^0 \nu \bar{\nu}$* . PhD thesis. SUNY Stonybrook (2000)
74. Kettell SH. In Ref. [27] (1999)
75. Lowe J. In Ref. [27] (1999)
76. Ecker G, et al. *Phys. Lett.* B189:363 (1987); Cappiello L, D'Ambrosio G. *Nuov. Cim.* 99A:153 (1988)
77. Barr GD, et al. *Phys. Lett.* B351:579 (1995)
78. Numao T. *Mod. Phys. Lett.* A7:3357 (1992)
79. Bergström L, Massó E, Singer P. *Phys. Lett.* B131:229 (1983)
80. Fanti V, et al. *Phys. Lett.* B458:553 (1999)
81. Barker AR. In Ref. [29] (2000)
82. Burkhardt H, et al. *Phys. Lett.* B199:139 (1987)
83. Barker AR. In Ref. [19] (1998)
84. Lath A. In Ref. [20] (1999)
85. Gjesdal S, et al. *Phys. Lett.* B44:217 (1973)
86. Angelopoulos A, et al. *Phys. Lett.* B413:232 (1997)
87. Alavi-Harati A, et al. *Phys. Rev. D* In press (2000); Yamanaka T. In Ref. [21] (1999)
88. Alavi-Harati A, et al. *Phys. Rev. D* In press (2000); also hep/ex-0001005 (2000)
89. Heiliger P, et al. *Phys. Rev. D* 47:4920 (1993)
90. Alavi-Harati A, et al. *Phys. Rev. Lett.* 83:917 (1999)
91. Contalbrigo M. In Ref. [30] (2000)
92. Ecker G, Pich A, de Rafael E. *Phys. Lett.* B237:481 (1990); Cheng HY. *Phys. Rev. D* 42:72 (1990); Bruno C, Prades J. *Z. Phys. C* 57:585 (1993)
93. Ecker G, Kambor J, Wyler D. *Nucl. Phys.* B394:101 (1993)
94. Ecker G, Pich A, de Rafael E. *Nucl. Phys.* B303:665 (1988)
95. Cappiello L, D'Ambrosio G, Miragliuolo M. *Phys. Lett.* B298:423 (1993); Cohen AG, Ecker G, Pich A. *Phys. Lett.* B304:347 (1993)
96. Kitching P, et al. *Phys. Rev. Lett.* 79:4079 (1997)
97. Taegar S. In Ref. [20] (1999)
98. Ecker G, Pich A, de Rafael E. *Nucl. Phys.* B291:692 (1987)
99. D'Ambrosio G, Ecker G, Isidori G, Portolés J. *J. High Energy Phys.* 8:4 (1998)

100. Bloch P, et al. *Phys. Lett.* B56:201 (1975)
101. Alliegro C, et al. *Phys. Rev. Lett.* 68:278 (1992)
102. Deshpande AL. *A study of the decay of a positively charged kaon into a positively charged pion, a positron and an electron, and a measurement of the decay of a neutral pion into a positron and an electron.* PhD thesis. Yale Univ. (1995)
103. Appel R, et al. *Phys. Rev. Lett.* 83:4482 (1999)
104. Adler S, et al. *Phys. Rev. Lett.* 79:4756 (1997)
105. Ma H, et al. *Phys. Rev. Lett.* 84:2580 (2000)
106. Kraus D. In Ref. [20] (1999)
107. D'Ambrosio G, Isidori G. *Z. Phys. C* 65:649 (1995); McGuigan M, Sanda AI. *Phys. Rev. D* 36:1413 (1987); Ecker G, Neufeld H, Pich A. *Phys. Lett.* B278:337 (1992); Ecker G, Neufeld H, Pich A. *Nucl. Phys.* B413:321 (1994); Lin YCR, Valencia G. *Phys. Rev. D* 37:143 (1988); Ko P, Truong TN. *Phys. Rev. D* 43:R4 (1991); Picciotto C. *Phys. Rev. D* 45:1569 (1992); Donoghue J, Holstein B, Lin YCR. *Nucl. Phys.* B277:651 (1986); He X, Valencia G. *Phys. Rev. D* 61:075003 (2000); Funck R, Kambor J. *Nucl. Phys.* B396:53 (1993); Heiliger P, Sehgal LM. *Phys. Lett.* B307:182 (1993)
108. Carrol A, et al. *Phys. Rev. Lett.* 44:529 (1980)
109. Taureg H, et al. *Phys. Lett.* B65:92 (1976)
110. Ramberg EJ, et al. *Phys. Rev. Lett.* 70:2525 (1993)
111. Belz J. In Ref. [22] (2000)
112. Abrams , et al. *Phys. Rev. Lett.* 29:1118 (1972)
113. Smith KM, et al. *Nucl. Phys.* B109:173 (1976)
114. Bolotov VN, et al. *Sov. J. Nucl. Phys.* 45:1023 (1987)
115. Adler S, et al. *Phys. Rev. Lett.* In press (2000); also hep-ex/0007021 (2000)
116. Sehgal LM, Wanniger M. *Phys. Rev. D* 46:1035; *Phys. Rev. D* 46:5209 (E) (1992)
117. Heiliger P, Sehgal LM. *Phys. Rev. D* 48:4146 (1993); Elwood JK, Wise MB, Savage MJ. *Phys. Rev. D* 52:5095 (1995); *Phys. Rev. D* 53:2855 (E) (1996); Elwood JK, Wise MB, Savage MJ, Walden JW. *Phys. Rev. D* 53:4078 (1996); Sehgal LM, van Leusen J. *Phys. Rev. Lett.* 83:4933 (1999)
118. Lubrano P. In Ref. [25] (2000)
119. Adams J, et al. *Phys. Rev. Lett.* 80:4123 (1998)
120. Barker AR. In Ref. [25] (2000); Senyo K. In Ref. [23] (2000)
121. Alavi-Harati A, et al. *Phys. Rev. Lett.* 84:408 (2000)
122. Contalbrigo M. In Ref [30]
123. Barr GD, et al. *Phys. Lett.* B328:528 (1994)
124. Donoghue J, Holstein B. *Phys. Rev. D* 50:3700 (1989); Ametller LI. *Phys. Lett.* B303:140 (1993)
125. Bijnens J, Ecker G, Gasser J. *Nucl. Phys.* B396:81 (1993)
126. Adler S, et al. *Phys. Rev. Lett.* In press (2000); also hep-ex/0003019 (2000)
127. Heintze J, et al. *Nucl. Phys.* B149:365 (1979)
128. Bijnens J, Talavera P. *Nucl. Phys.* B489:387 (1997)
129. Akiba Y, et al. *Phys. Rev. D* 32:2911 (1985)
130. Poblaguev A, private communication; Zeller M. In Ref. [24] (2000)
131. Ma H, private communication
132. Atiya MS, et al. *Phys. Rev. Lett.* 63:2177 (1989)
133. Adler S, et al. *Phys. Rev. D* 58:012003-1 (1998)
134. Weinberg S. *Phys. Rev. Lett.* 17:616 (1966); Gasser J, Leutwyler H. *Phys. Lett.* B125:325 (1983)
135. Bijnens J, et al. *Phys. Lett.* B374:210 (1996); Knecht M, Moussallam B, Stern J, Fuchs NH. *Nucl. Phys.* B457:513 (1995); Bijnens J, et al. *Nucl. Phys.* B508:263 (1997); Amoros J, Bijnens J. *J. Phys.* G25:1607 (1999); Amoros J, Bijnens J, Talavera P. hep-ph/9912398 (1999)
136. Rosselet L, et al. *Phys. Rev. D* 15:574 (1977)
137. Pislak S. *Proc. Workshop on Hadronic Atoms, Bern, Oct. 1999*
138. Schenk A. *Nucl. Phys.* B363:97 (1991); Ananthanarayan B, Colangelo G, Gasser J, Leutwyler H. hep-ph/0005297 (2000)
139. Pislak S, private communication
140. Basdevant JL, Froggatt CD, Petersen JL. *Nucl. Phys.* B72:413 (1974)
141. Bisi V, Cester R, Chiesa AM, Vigone M. *Phys. Lett.* B25:572 (1967)

142. Makoff G, et al. *Phys. Rev. Lett.* 70:1591 (1993)
143. Barmin VV, et al. *Sov. J. Nucl. Phys.* 48:1032 (1988)
144. Barmin VV, et al. *Sov. J. Nucl. Phys.* 55:547 (1992)
145. Adler R, et al. *Phys. Lett.* B407:193 (1997)
146. Achasov, MN et al. *Phys. Lett.* B459:674 (1999)
147. Barmin VV, et al. *Sov. J. Nucl. Phys.* 50:421 (1989)
148. Bolotov VN, et al. *J. Exp. Theor. Phys. Lett.* 42:481 (1995)
149. Ljung D, Cline D. *Phys. Rev. D* 8:1307 (1973)
150. Bender M, et al. *Phys. Lett.* B418:411 (1998)
151. Barmin VV, et al. *Sov. J. Nucl. Phys.* 53:606 (1991)
152. Bolotov VN, et al. *Sov. J. Nucl. Phys.* 44:68 (1986)
153. Leber F, et al. *Phys. Lett.* B369:69 (1996)
154. Wilczek F, Zee A. *Phys. Rev. Lett.* 42:421 (1979); Cahn R, Harari H. *Nucl. Phys.* B176:135 (1980)
155. Eichten E, Lane K. *Phys. Lett.* B90:125 (1980); Dimopoulos S, Ellis J. *Nucl. Phys.* B182:505 (1981); Shanker O. *Nucl. Phys.* B206:253 (1982); Haber HE, Kane GL. *Phys. Rep.* 117:75 (1985); Bigi II. *Phys. Lett.* B166:238 (1986); Pati J, Stremnitzer H. *Phys. Lett.* B172:441 (1986); Campbell BA, et al. *Int. J. Mod. Phys.* A2:831 (1987); Langacker P, Sankar SU, Schilcher K. *Phys. Rev. D* 38:2841 (1988); Mukhopadhyaya B, Raychaudhuri A. *Phys. Rev. D* 42:3515 (1990); Gagyi-Palfy Z, Pilaftsis A, Schilcher K. *Nucl. Phys.* B513:517 (1998)
156. Greenlee HB, et al. *Phys. Rev. Lett.* 60:893 (1988); Schaffner SF, et al. *Phys. Rev. D* 39:990 (1989)
157. Cousins RD, et al. *Phys. Rev. D* 38:2914 (1988); Mathiazhagan C, et al. *Phys. Rev. Lett.* 63:2181 (1989); Arisaka K, et al. *Phys. Rev. Lett.* 70:1049 (1993)
158. Inagaki T, et al. *Phys. Rev. D* 40:1712 (1989); Akagi T, et al. *Phys. Rev. Lett.* 67:2614 (1991); Akagi T, et al. *Phys. Rev. D* 51:2061 (1995)
159. Ambrose D, et al. *Phys. Rev. Lett.* 81:5734 (1998)
160. Bergman DR. *A search for the decay $K^+ \rightarrow \pi^+ \mu^+ e^-$* . PhD thesis. Yale Univ. (1998); Pislak S. *Experiment E865 at BNL: a search for the decay $K^+ \rightarrow \pi^+ \mu^+ e^-$* . PhD thesis. Univ. Zürich (1998)
161. Lee AM, et al. *Phys. Rev. Lett.* 64:165 (1990); Campagnari C, et al. *Phys. Rev. Lett.* 61:2062 (1988); Baker NJ, et al. *Phys. Rev. Lett.* 59:2832 (1987)
162. Appel R, et al. *Phys. Rev. Lett.* In press (2000); also hep-ex/0005016 (2000); Zeller M. In Ref. [24] (2000)
163. Arisaka K, et al. *Phys. Lett.* B432:230 (1998)
164. Appel R, et al. *Phys. Rev. Lett.* In press (2000); also hep-ex/0006003 (2000)
165. Gu P, et al. *Phys. Rev. Lett.* 76:4312 (1996)
166. Deshpande A, et al. *Phys. Rev. Lett.* 71:27 (1993)
167. Appel R, et al. *Nucl. Instrum. Methods Phys. Res., Sect. A* In press (2000)
168. Lee DM, et al. *Nucl. Instrum. Methods Phys. Res., Sect. A* 256:329 (1987); Kenney CJ, et al. *IEEE Trans. Nucl. Sci.* 36:74 (1989); Frank J, et al. *IEEE Trans. Nucl. Sci.* 36:79 (1989); Cousins RD, et al. *IEEE Trans. Nucl. Sci.* 36:646 (1989); Biery KA, et al. *IEEE Trans. Nucl. Sci.* 36:650 (1989); Cousins RD, et al. *Nucl. Instrum. Methods Phys. Res., Sect. A* 277:517 (1989)
169. Mathiazhagan C, et al. *Phys. Rev. Lett.* 63:2185 (1989); Heinson AP, et al. *Phys. Rev. D* 44:R1 (1991); Arisaka K, et al. *Phys. Rev. Lett.* 71:3910 (1993); Heinson AP, et al. *Phys. Rev. D* 51:985 (1995)
170. Belz J, et al. *Nucl. Instrum. Methods Phys. Res., Sect. A* 428:239 (1999)
171. Ahmad S, et al. *IEEE Trans. Nucl. Sci.* 33:178 (1986); Cresswell JV, et al. *IEEE Trans. Nucl. Sci.* 35:460 (1988); Atiya MS, et al. *IEEE Trans. Nucl. Sci.* 36:813 (1989); Atiya MS, et al. *Nucl. Instrum. Methods Phys. Res., Sect. A* 279:180 (1989); Atiya MS, et al. *Nucl. Instrum. Methods Phys. Res., Sect. A* 321:129 (1992)
172. Atiya MS, et al. *Phys. Rev. Lett.* 64:21 (1990); Atiya MS, et al. *Nucl. Phys. B Proc. Suppl.* 13:568 (1990); Atiya MS, et al. *Phys. Rev. Lett.* 65:1188 (1990); Atiya MS, et al. *Phys. Rev. Lett.* 66:2189 (1991); Atiya MS, et al. *Phys. Rev. Lett.* 69:733 (1992); Atiya MS, et al. *Nucl. Phys.* A527:727c (1991); Atiya MS, et al. *Phys. Rev. Lett.* 70:2521 (1993); Atiya MS, et al. *Phys. Rev. D* 48:R1 (1993); Adler S, et al. *Phys. Rev. Lett.* 76:1421 (1996)
173. Burke M, et al. *IEEE Trans. Nucl. Sci.* 41:131 (1946); Kobayashi M, et al. *Nucl. Instrum.*

- Methods Phys. Res., Sect. A* 337:355 (1994); Chiang IH, et al. *IEEE Trans. Nucl. Sci.* 42:394 (1995); Bryman DA, et al. *Nucl. Instrum. Methods Phys. Res., Sect. A* 396:394 (1997); Komatsubara TK, et al. *Nucl. Instrum. Methods Phys. Res., Sect. A* 404:315 (1998); Blackmore EW, et al. *Nucl. Instrum. Methods Phys. Res., Sect. A* 404:295 (1998); Doornbos J, et al. *Nucl. Instrum. Methods Phys. Res., Sect. A* 444:546 (2000)
174. Papadimitriou V, et al. *Phys. Rev. D* 44:573 (1991); Graham G, et al. *Phys. Lett.* B295:169 (1992); Krolak P, et al. *Phys. Lett.* B320:407 (1994); Gu P, et al. *Phys. Rev. Lett.* 72:3000 (1994); Weaver M, et al. *Phys. Rev. Lett.* 72:3758 (1994); Roberts D, et al. *Phys. Rev. D* 50:1874 (1994); Nakaya T, et al. *Phys. Rev. Lett.* 73:2169 (1994)
175. Whitmore J. *Nucl. Instrum. Methods Phys. Res., Sect. A* 409:687 (1998); Bown C, et al. *Nucl. Instrum. Methods Phys. Res., Sect. A* 369:248 (1996)
176. Burkhardt H, et al. *Nucl. Instrum. Methods Phys. Res., Sect. A* 268:116 (1988); Barr GD, et al. *IEEE Trans. Nucl. Sci.* 36:66 (1989); Barr G, et al. *Nucl. Instrum. Methods Phys. Res., Sect. A* 294:465 (1990)
177. Barr GD, et al. *Phys. Lett.* B235:356 (1990); Barr GD, et al. *Phys. Lett.* B240:283 (1990); Barr GD, et al. *Phys. Lett.* B242:523 (1990); Barr GD, et al. *Phys. Lett.* B259:389 (1991); Barr GD, et al. *Phys. Lett.* B284:440 (1992); Kreutz A, et al. *Z. Phys. C* 65:67 (1995); Barr GD, et al. *Z. Phys. C* 65:361 (1995); Barr GD, et al. *Phys. Lett.* B358:339 (1995)
178. Buchholz P, et al. *Nucl. Instrum. Methods Phys. Res., Sect. A* 316:1 (1992); Barr GD, et al. *Nucl. Instrum. Methods Phys. Res., Sect. A* 323:393 (1992); Fanti V, et al. *Nucl. Instrum. Methods Phys. Res., Sect. A* 344:507 (1994); Ceccucci A, et al. *Nucl. Instrum. Methods Phys. Res., Sect. A* 360:224 (1995); Barr GD, et al. *Nucl. Instrum. Methods Phys. Res., Sect. A* 370:413 (1996); Gorini B, et al. *IEEE Trans. Nucl. Sci.* 45:1771 (1998); Anvar S, et al. *Nucl. Instrum. Methods Phys. Res., Sect. A* 419:686 (1998); Bergauer H, et al. *Nucl. Instrum. Methods Phys. Res., Sect. A* 419:623 (1998); Hallgren B, et al. *Nucl. Instrum. Methods Phys. Res., Sect. A* 419:680 (1998); Fischer G, et al. *Nucl. Instrum. Methods Phys. Res., Sect. A* 419:695 (1998); Schinzel D, et al. *Nucl. Instrum. Methods Phys. Res., Sect. A* 419:217 (1998); Palestini S, et al. *Nucl. Instrum. Methods Phys. Res., Sect. A* 421:75 (1998)
179. Fanti V, et al. *Z. Phys. C* 76:653 (1998)
180. Finocchiaro G, et al. *Nucl. Instrum. Methods Phys. Res., Sect. A* 360:48 (1997); Franzini J, et al. *Nucl. Instrum. Methods Phys. Res., Sect. A* 360:201 (1997); Calcaterra A, et al. *Nucl. Instrum. Methods Phys. Res., Sect. A* 367:104 (1997); Grangnolo F, et al. *Nucl. Instrum. Methods Phys. Res., Sect. A* 367:108 (1997); Antonelli M, et al. *Nucl. Instrum. Methods Phys. Res., Sect. A* 368:352 (1997); Bossi F, et al. *Nucl. Instrum. Methods Phys. Res., Sect. A* 379:536 (1997); Antonelli M, et al. *Nucl. Phys. B Proc. Suppl.* 54:14 (1997); Dell'Agnello S, et al. *Nucl. Phys. B Proc. Suppl.* 54:57 (1997); Elia V, et al. *Nucl. Phys. B Proc. Suppl.* 54:66 (1997); Spagnolo S, et al. *Nucl. Phys. B Proc. Suppl.* 54:70 (1997); Lacava F, et al. *Nucl. Phys. B Proc. Suppl.* 54:327 (1997)
181. Landsberg L. In Ref. [24] (2000)
182. Akagi T, et al. *Phys. Rev. Lett.* 67:2618 (1991)
183. Akagi T, et al. *Phys. Rev. D* 47:R2644 (1993)
184. Nomura T, et al. *Phys. Lett.* B408:445 (1997); Takeuchi Y, et al. *Phys. Lett.* B443:409 (1998)
185. Murakami K, et al. *Phys. Lett.* B463:333 (1999)